Reflection analysis of non-linear regular waves

Mansard, E.; Sand, S.; Funke, E.

Publisher's version / Version de l'éditeur:

Technical Report (National Research Council of Canada. Hydraulics Laboratory); no. TR-HY-011, 1985

UNLIMITED
UNCLASSIFIED

ILLIMITÉ
NON CLASSIFIÉ

Technical Report

Rapport technique

1985/11

TR-HY-011
NRC NO. 25144

REFLECTION ANALYSIS OF NON-LINEAR REGULAR WAVES

E.P.D. Mansard, S.E. Sand, E.R. Funke

Division of
Mechanical Engineering

Division de
génie mécanique

National Research
Council Canada

Conseil national
de recherches Canada

Canada

UNLIMITED
UNCLASSIFIED

ILLIMITÉ
NON CLASSIFIÉ

REFLECTION ANALYSIS OF NON-LINEAR REGULAR WAVES

ANALYSE DE RÉFLEXION DES HOULES RÉGULÈRES NON-LINÉAIRES

E. P. D. Mansard, S. E. Sand and E. R. Funke

Technical Report

Rapport technique

1985/11

TR-HY-011
NRC No. 25144

J. Ploeg, Head/Chef
Hydraulics Laboratory/
Laboratoire d'hydraulique

E.H. Dudgeon
Director/
Directeur

ACKNOWLEDGEMENTS

Miss Deborah Bouck from DMR Associates Ltd. has coded and tested all of the computer programs which are part of the monochromatic reflection analysis package. Her competence, perseverance and patience contributed significantly to the conclusion of the study.

ABSTRACT

Conventional reflection analyses assume that all waves propagate with celerities described by the 1st-order linear dispersion theory. However, finite amplitude waves are known to bind a certain amount of 2nd harmonic energy which travels with the celerity of the fundamental. When these waves are simulated in a laboratory using the classical 1st-order generation, they produce additional 2nd-order free parasitic waves. The bound and free components have different celerities and therefore they cannot be analysed by the conventional analysis. This report presents a non-linear reflection analysis technique which can separate these bound and free components. This technique is different from the Fourier approach and it is based on optimal fitting of sinusoids to the measured time series. Extensive numerical simulation has been used to validate this technique with both linear and non-linear regular waves.

RÉSUMÉ

Dans l'analyse conventionnelle de réflexion on suppose que toutes les composantes de houles se propagent avec leurs propres célérités; mais dans le cas des houles d'amplitude finie, il existe une composante d'harmonique de fréquence double qui est rattachée à la fondamentale et se propage à la même célérité que la fondamentale. Quand ces houles sont engendrées dans un canal à houle par la méthode classique de génération (génération du 1er ordre) des composantes du 2ème ordre, également de double fréquence, sont introduites. Ces composantes dites "houles parasites" ne sont pas rattachées à leur fondamentale et se propagent donc suivant la loi de dispersion linéaire. Comme ces composantes rattachées et non-rattachées ont des célérités différentes, l'analyse classique de réflexion ne peut offrir une estimation correcte. Ce document présente une nouvelle approche non-linéaire qui peut identifier les composantes rattachées et non-rattachées dans un système de clapotis. Cette méthode n'utilise pas l'analyse de Fourier, mais par contre elle utilise une technique qui ajuste d'une façon optimale des sinusoïdes. Une simulation numérique détaillée a été utilisée afin de valider cette nouvelle méthode avec des houles régulières linéaires ainsi que non-linéaires.

CONTENTS

LIST OF ILLUSTRATIONS

LIST OF TABLES

LIST OF SYMBOLS

Symbol	Meaning	Units
A	Amplitude of the wave	m
A_i	Amplitude of the incident wave	m
A_r	Amplitude of the reflected wave	m
C	Celerity of the fundamental wave	m/s
C_f	Celerity of the 2nd-order free component	m/s
C_r	Reflection coefficient	
$C_{r,b}$	Reflection coefficient of the bounded component	
$C_{r,f}$	Reflection coefficient of the free component	
$C'_{r,b}$	Mean reflection coefficient (fundamental + bound)	
$C'_{r,f}$	Mean reflection coefficient (fundamental + free)	
f	Frequency of the wave	Hz
F_1	Transfer function for 2nd-order wave generation	
F_{23}	Transfer function for 2nd-order wave generation	
G^+	Non-linear transfer function for 2nd harmonic waves	1/m
h	Water depth	m
$H^{(1)}$	1st-order wave height	m
$H_{HB}^{(2)}$	2nd-order wave height of the bound component	m
$H_f^{(2)}$	2nd-order wave height of the free wave	m
H_i	Incident wave height	m
H_r	Reflected wave height	m
H_1	Wave height at an antinode of the standing wave system	m
H_2	Wave height at a node of the standing wave system	m
k	Wave number	rad/m

LIST OF SYMBOLS (Cont'd)

Symbol	Meaning	Units
L_0	Deep water wave length	m
L_x	Wave length of spatial variation of wave height	m
p	Index of the probe	
T	Period of the wave	s
X	Spatial variable, positive in the direction of propagation of the incident wave	m
X_T	Total length of the flume	m
X_{12}	Spacing between probes 1 and 2	m
X_{13}	Spacing between probes 1 and 3	m
$X^{(1)}(t)$	Time series of the 1st-order control signal	m
$X^{(2)}(t)$	Time series of the 2nd-order control signal	m
α	Magnitude of the noise level	%
β	Reflection coefficient used in the synthesis	
ϕ_i	Phase of the incident wave	rad
ϕ_r	Phase of the reflected wave	rad
$\eta^{(1)}(t)$	Time series of the 1st-order waver surface elevation	m
$\eta(X,t)$	Time series of the water surface elevation at a distance X from the paddle	m
$\eta_1(t)$, $\eta_2(t)$, $\eta_3(t)$	Time series of the water surface elevation at probes 1, 2 and 3 respectively	m
η_f	Elevation of the free wave component	m
η_{HB}	Elevation of the bound wave component	m
η_C	Crest elevation	m
ω	Cyclic frequency	rad/s

REFLECTION ANALYSIS OF NON-LINEAR REGULAR WAVES

1.0 INTRODUCTION

In many laboratories, design of beaches is often part of a continuous research program which is aimed at developing an efficient wave absorbing device. Ideally, such a device should be small in its length ensuring at the same time effective dissipation of energy for a large number of frequency components. The performance of the various absorbers is generally evaluated by measuring the reflected wave energy. For instance, if A_i^2 is the energy of the incident wave, the following expression can be written, through energy balance:

$$A_i^2 = A_r^2 + E_{LOSS} \tag{1}$$

where A_r^2 is the reflected energy, and

E_{LOSS} is the energy dissipated by the structure.

It therefore follows that the lower the reflected energy is, the better is the performance of the absorber. Many techniques exist for the measurement of reflected energy and this energy is often expressed in terms of the reflection coefficient. The reflection coefficient, C_r, is defined as the ratio of wave height reflected by the absorber over the incident wave height generated by the paddle.

At present, most of these reflection analysis techniques are based on linear theory, which corresponds to "small" amplitude waves. Although this linear theory is satisfactory for a wide range of wave heights a higher order theory, which can deal with various non-linearities in the waves, is urgently needed. This report presents a new technique, based on 2nd-order theory, which can deal with one of many aspects of non-linearities (i.e. interaction of 2nd-order free and bound harmonics). The theoretical background and the implementation of this technique for the case of regular waves are described here and an extension of this method for an irregular sea state is underway.

2.0 REFLECTION ANALYSIS - A BRIEF REVIEW

The conventional reflection analysis is based on measurements of nodes and antinodes of the standing wave system set-up by a given structure. If H_1 and H_2 are the wave heights measured at an antinode and a node respectively, the reflection coefficient C_r is equal to:

$$C_r = \frac{H_1-H_2}{H_1+H_2} \tag{2}$$

The values of H_1 and H_2 can be obtained either:

(1) by measuring the envelope of the standing wave system, say by a moving carriage, and use the maxima and the minima of the envelope as H_1 and H_2, recpectively, or,

(2) by detecting the positions of maxima and minima in the flume and measure their respective heights.

However, this method, which is based on monochromatic waves, cannot be used for an irregular sea state due to the large number of frequency components involved. Since many hydraulic laboratories now have the capability of testing structures with irregular waves, the measurement of reflections in an irregular sea state has become more of a necessity. The commonly used technique for this purpose, is the 2-probe method proposed by Thornton and Calhoun [Ref. 12], Goda and Suzuki [Ref. 5] and Morden et al. [Ref. 8]. The Hydraulics Laboratory of NRCC uses a 3-probe method for estimating the reflections in a least squares sense (Mansard and Funke [Ref. 6]).

The 2-probe and 3-probe methods are basically the same: they both consist of simultaneous measurements of the co-existing waves (sum of incident and reflected waves) at two or three known positions (depending on the method) in a line parallel to the direction of propagation. Fourier analysis of these measurements then provides the amplitudes and phases of the frequency components constituting the irregular sea state, on the basis of which the incident and reflected components could be resolved. An alternative to this approach is to use spectral analysis (auto and cross-spectral analyses) instead of the Fourier analysis and determine the reflection of frequency bands rather than of each individual frequency component. This approach has been evaluated by numerical simulations and found to give reliable estimations of the reflections. At the same time, this latter approach does also eliminate erratic variations of reflection coefficients which are caused by frequency components with little or no energy (Mansard and Funke [Ref. 7]).

The methods described above for irregular waves are also applicable for regular waves, although their inability to define the frequency of the monochromatic wave precisely is a source of error.

2.1 REFLM - Reflection Analysis of Monochromatic Waves

The Hydraulics Laboratory of NRCC has recently developed a program REFLM for estimating the reflection of monochromatic waves. This program, which is based on the 3-probe method, has the unique capability of fitting a sinusoid in a least squares sense to each of the three regular wave time series. This technique is superior to a Fourier transform method as it computes precisely the fundamental frequency, amplitude and phase, whereas the Fourier method is extremely sensitive to the truncation length of the wave record in relation to the period of the wave being analysed. In fact, previous application of cross-spectral density techniques to monochromatic waves resulted in a number of unexplained inconsistencies, which were probably a function of the resolution, filter limits and location of probe array relative to the wave paddle. However, this newly developed technique certainly checks out well with simulated data and, as shown in the next section, it appears to be relatively independent of probe location.

Although this program is based on a least squares fitting of sinusoids, it still uses the least square method for separating the incident and the reflected components as deployed for irregular waves (Mansard and Funke [Ref. 6]).

2.2 Testing of REFLM by Numerical Simulations

In order to validate the program REFLM, extensive series of tests were carried out using numerical simulations. Time series of monochromatic waves with known incident and reflected characteristics were simulated for three hypothetical probe positions. The equations used in the simulations are basically similar to those presented in Mansard and Funke [Ref. 7] for irregular waves. As in the case of irregular waves, the simulation program had the flexibility of incorporating a certain noise level in the time series, in order to represent the noise and measurement errors which generally prevail in an experimental set-up. The noise signal was generated by a Gaussian, "white" random number generator and its magnitude was expressed in terms of percentage of the RMS value of the incident wave.

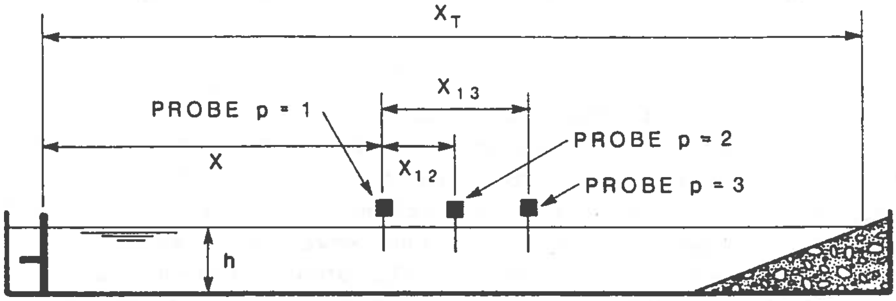

FIGURE 1 DEFINITION SKETCH FOR THE REFLECTION SIMULATION

Figure 1 illustrates the concept used in the simulations, for which the time series $\eta(X,t)$ can be written as:

$$\eta(X,t) = A_i * \{\cos\left[\frac{2\pi(i-1)t}{T} - \frac{2\pi X}{L}\right] + \beta * \cos\left[\frac{2\pi(i-1)t}{T} - \frac{2\pi(2X_T - X)}{L}\right]$$

$$+ .707\alpha * \mathrm{RANDG(SEED,1)}\}$$

where A_i is the amplitude of the incident wave,

L and T are the wave length and period of the wave, respectively,

β is the reflection coefficient, and

α is the magnitude of the noise.

In particular for $X = 0$, the equations for probes $p = 1$, $p = 2$ and $p = 3$ can be written as:

$$\eta_1(t) = \eta(0,t) = A_i * \left\{\cos\left[\frac{2\pi\cdot(i-1)\cdot t}{T}\right] + \beta*\cos\left[\frac{2\pi\cdot(i-1)\cdot t}{T} - \frac{2\pi(2X_T)}{L}\right] + .707\alpha*\mathrm{RANDG(SEED,1)}\right\} \tag{3}$$

$$\eta_2(t) = \eta(X_{12},t) = A_i * \left\{\cos\left[\frac{2\pi\cdot(i-1)\cdot t}{T} - \frac{2\pi\cdot X_{12}}{L}\right] + \beta*\cos\left[\frac{2\pi\cdot(i-1)\cdot t}{T} - \frac{2\pi(2X_T-X_{12})}{L}\right] + .707\alpha*\mathrm{RANDG(SEED,1)}\right\} \tag{4}$$

and $$\eta_3(t) = \eta(X_{13},t) = A_i * \left\{\cos\left[\frac{2\pi\cdot(i-1)\cdot t}{T} - \frac{2\pi X_{13}}{L}\right] + \beta*\cos\left[\frac{2\pi\cdot(i-1)\cdot t}{T} - \frac{2\pi\cdot(2X_T-X_{13})}{L}\right] + .707\alpha*\mathrm{RANDG(SEED,1)}\right\} \tag{5}$$

The results of the numerical simulations are summarized in Tables 1 and 2, wherein the resolved incident and reflected heights are presented along with the reflection coefficients. Often, the reflection coefficient, which is the ratio of reflected to incident wave height tends to show more variability than the wave heights. Table 1, which illustrates the effect of a noise signal, shows that satisfactory estimation of reflections can be obtained even with 20% noise. It also shows that the smaller the reflected wave height is, the larger is the deviation from the true value due to the high noise/signal ratio.

In order to evaluate the effect of probe location in a flume a similar set of simulations were carried out with two other locations of the probes in the flume [see X in Fig. 1]. The results are summarized in Table 2 and they show, as expected, that the reflection coefficient is independent of the probe location, although there are small discrepancies due to minor differences in the optimal fitting of the time series. By choosing different locations in the flume, the phases and amplitudes of the standing wave system are changed with respect to the Gaussian distribution of the noise level. A comparable operation would have been to modify the distribution of the noise with respect to a fixed set of amplitudes and phases. Hence, it is expected that the differences found in Table 2 are due to variability of the noise distribution, which in turn affects the optimal fitting of sinusoids. In general, different types of noise may result in different variability of the reflections. However, since the character of the noise which actually prevails in an experimental set-up is unknown, Table 2 is believed to give a useful indication of the variability.

NOISE	INCIDENT HEIGHT		REFLECTED HEIGHT		REFLECTION COEFFICIENT	
α*100 %	EXPECTED (m)	COMPUTED (m)	EXPECTED (m)	COMPUTED (m)	EXPECTED %	COMPUTED %
0	.1200	.1200	.0024	.0024	2.00	2.00
1		.1200		.0024		2.03
5		.1202		.0026		2.18
10		.1203		.0029		2.37
15		.1205		.0031		2.56
20		.1206		.0033		2.75
0	.1200	.1200	.0240	.0240	20.00	20.00
1		.1200		.0241		20.04
5		.1202		.0243		20.19
10		.1203		.0245		20.38
15		.1205		.0248		20.57
20		.1207		.0248		20.52

TABLE 1 RESULTS OF NUMERICAL SIMULATIONS FOR X = 0

2.3 Outputs of REFLM

An example of the reflection analysis results from REFLM is given in Figures 2 and 3 for the case with 10% noise and 20% reflection. Figure 2 displays the original time series synthesized for the three probe positions (x_{12} = 0.40 m, X_{13} = 0.66 m; see Fig. 1 for definition of X_{12} and X_{13}). For comparison, the optimally fit time series for the above cases are also presented in the same figure. As indicated above, the program REFLM estimates the best combination of frequency, amplitude and phase (three parameter fitting) for the description of the synthesized time series (in a least squares sense). However, this fitting technique, which is based on the Gauss-Newton method, requires initial guesses of these three parameters. These initial guesses are internally calculated by a zero crossing analysis. An alternative method of determining the initial guesses is by FFT analysis, but this may be more suitable for an irregular sea state. As an example, the outputs of the fitting technique are given below for this particular case.

NOISE α*100 %	INCIDENT HEIGHT			REFLECTED HEIGHT			REFLECTION COEFFICIENT		
	X = 0	X = 5	X = 20	X = 0	X = 5	X = 20	X = 0	X = 5	X = 20
0	.1200	.1200	.1200	.0024	.0024	.0024	2.00	2.01	1.99
1	.1200	.1200	.1200	.0024	.0024	.0024	2.03	1.97	2.00
5	.1202	.1198	.1199	.0026	.0022	.0024	2.18	1.84	2.03
10	.1203	.1198	.1198	.0029	.0020	.0025	2.37	1.70	2.07
15	.1205	.1196	.1196	.0031	.0019	.0025	2.56	1.57	2.12
20	.1206	.1195	.1195	.0033	.0018	.0026	2.75	1.47	2.19
0	.1200	.1200	.1200	.0240	.0240	.0240	20.00	20.00	20.00
1	.1200	.1200	.1200	.0241	.0240	.0240	20.04	19.98	20.01
5	.1202	.1199	.1199	.0243	.0238	.0241	20.19	19.88	20.07
10	.1203	.1198	.1197	.0245	.0237	.0241	20.38	19.76	20.13
15	.1205	.1196	.1196	.0248	.0235	.0241	20.57	19.63	20.17
20	.1207	.1195	.1194	.0248	.0233	.0242	20.52	19.52	20.23

TABLE 2 NUMERICAL SIMULATIONS OF THE EFFECTS OF PROBE LOCATION

	AMPLITUDE	PHASE	FREQUENCY
FITTING OF PROBE 1			
Initial guesses	.06529	1.67102	.55496
Fitted values	.06333	1.75817	.55501
FITTING OF PROBE 2			
Initial guesses	.05136	0.89800	.55497
Fitted values	.04874	0.95499	.55498
FITTING OF PROBE 3			
Initial guesses	.05297	0.25784	.55501
Fitted values	.05048	0.27256	.55502

Figure 3 illustrates the main output of the reflection analysis. This output is similar to the one used by NRCC for the analysis of irregular waves (Mansard and Funke [Ref. 7]).

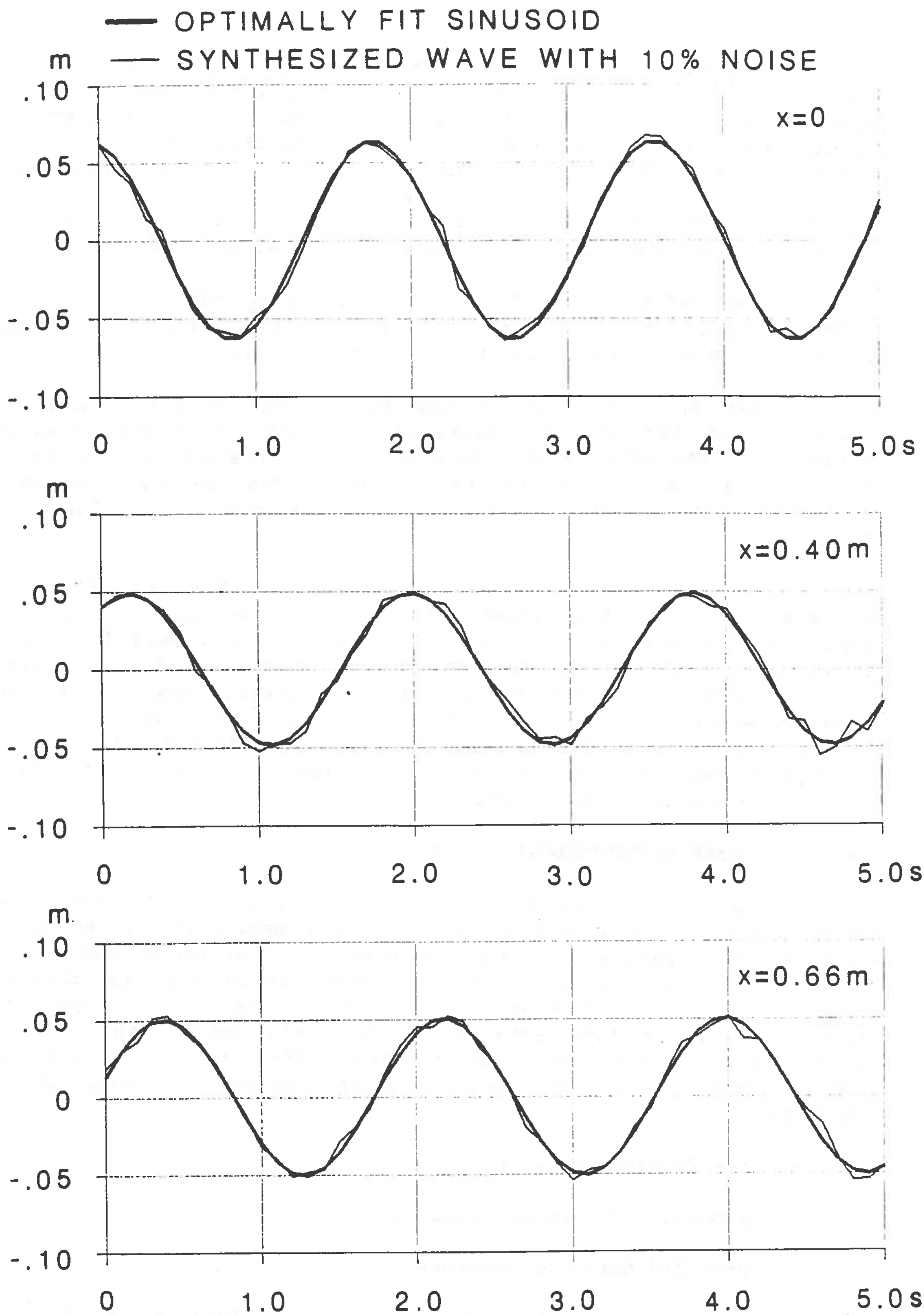

FIGURE 2 FITTING OF SINUSOIDS TO SYNTHESIZED TIME SERIES

Figure 3a presents the auto-spectrum of the first probe along with incident and reflected spectra resolved by the analysis. A rectangular display of these spectra is given in order to maintain compatibility with the outputs from irregular waves. The area under the rectangle is adjusted to be equivalent to the variance of the monochromatic wave.

Figure 3b gives the auto-spectra of the three time series corresponding to the three probes used in the reflection analysis.

The reflection coefficient estimated by the analysis is displayed in Figure 3c while an indication of the reliability of the analysis results is provided by the error function given in Figure 3e.

The error function is the square root of the minimum least squares error between the measured and the estimated co-existing incident and reflected waves, normalized with respect to the incident wave. It is therefore a measure of the residual between the measured and the estimated quantities and is an indicator of the quality of the analysis.

The coherency function is generally a function of frequency and is a measure of the linear interdependence between two time functions. For monochromatic waves the coherency is always 1 unless the variances of a pair of signals is averaged over a band of frequencies which can account for the corrupting noise power. However, for monochromatic waves the value of the coherency would be highly dependent on the arbitrary choice of this band width and therefore fails to serve as an adequate measure of noise corruption. For this reason the coherency value in Figure 3d is always set to 1.

3.0 NON-LINEAR REFLECTION ANALYSIS

As demonstrated by Stokes [Ref. 11], a regular wave is never purely linear. It always binds a certain amount of higher harmonic energy which propagates with the fundamental. Therefore, when computing the reflection on the basis of the assumption of a linear dispersion relation, errors are inevitably introduced. The linear dispersion is valid only for the fundamental wave component, whereas the bound part (of double frequency) should be treated differently. As outlined in Sand and Mansard [Ref. 10], regular waves measured in a flume are composed of:

- the fundamental wave,
- a bound 2nd harmonic component,
- free 2nd harmonic components, and
- higher harmonics which are treated here as part of the residual noise.

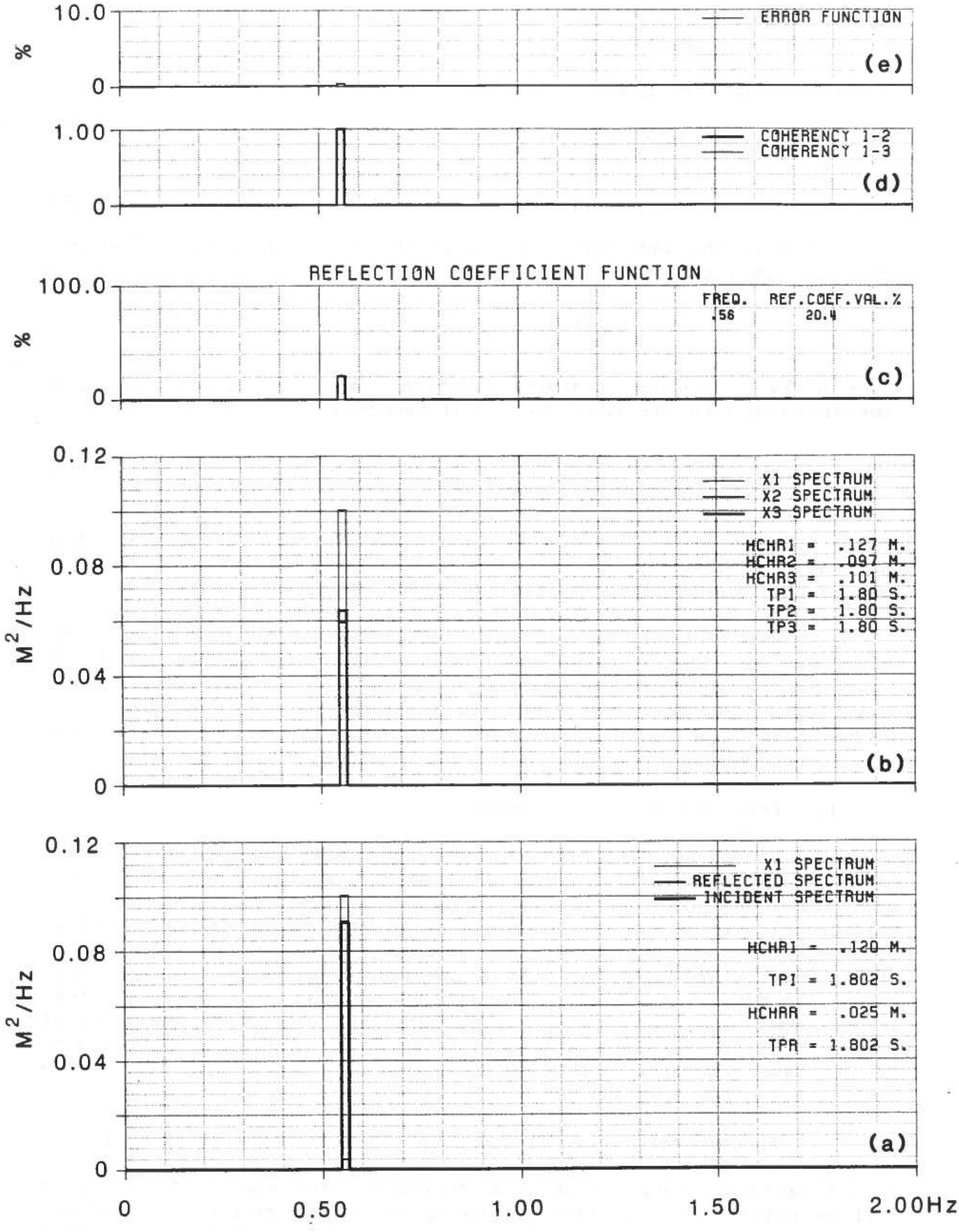

FIGURE 3 OUTPUT OF REFLECTION ANALYSIS

The calculation of the bound and the free wave parts will be discussed in the following sections.

3.1 Bound 2nd Harmonic Component

If the fundamental, regular wave is given as:

$$\eta^{(1)}(t) = A \cos(\omega t) \tag{6}$$

in which A is the wave amplitude, ω is the cyclic frequency, $\omega = 2\pi f$, and t the time, then the bound 2nd-order part is:

$$\eta_{HB}^{(2)}(t) = A^2 G^+ \cos(2\omega t) \tag{7}$$

where G^+ is a 2nd-order transfer function. When this function is made dimensionless with the water depth h it becomes:

$$G^+ h = \frac{1}{4} kh \frac{\cosh kh}{\sinh^3 kh} (1+2 \cosh^2 kh) \tag{8}$$

and it is plotted in Figure 4 as a function of h/L_0, L_0 being the deep water wave length. It is seen from the figure that the 2nd harmonic component is significant, especially in shallow water areas.

When the fundamental wave amplitude and frequency are given it is now possible, from equation (8) or the graph in Figure 4, to determine the bound wave component. It is important to note that no matter what type of control signal is used for the wave generation (1st or 2nd-order), the bound 2nd harmonic component will always exist in the wave flume.

3.2 Free Second Harmonic Waves

When generating regular waves in a wave basin or a flume, it is common to encounter a significant amount of free, second harmonic wave activity. This originates from two sources. One is that the traditional wave generation technique which uses only a 1st order transfer function does not satisfy the necessary 2nd-order boundary conditions for the 2nd harmonic. This inevitably produces undesired free waves (for details see Sand and Mansard [Ref. 10]). The amount of free, second order wave energy which is so generated depends on the depth of water, on the height and the length of the fundamental wave and the mode of the wave generator. This is described in Figure 5 in terms of a ratio between the free and the bound, second harmonic wave height.

Another reason may be found in the reflection process itself. If a portion of the fundamental wave is reflected, then the amount of second harmonic energy which this reflected wave must bind to itself will be reduced in proportion to the square of its amplitude as indicated by equation (7). Any excess in the 2nd harmonic energy which cannot be bound to the reflected fundamental must therefore be presumed to be released as free 2nd harmonic energy.

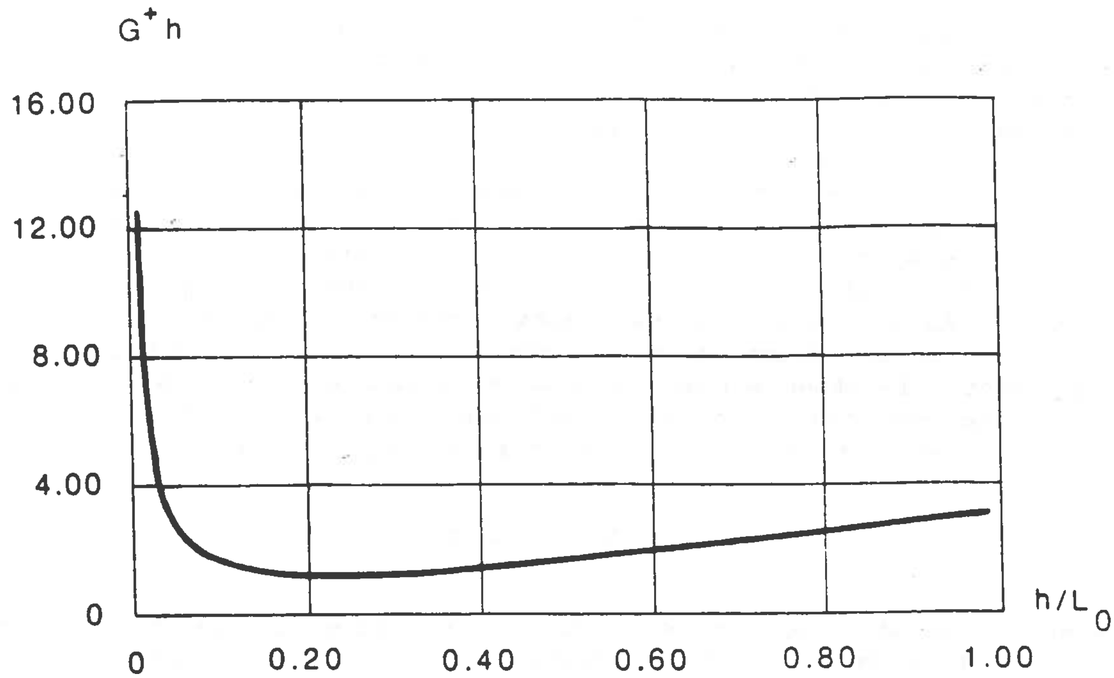

FIGURE 4 TRANSFER FUNCTION FOR 2nd HARMONICS

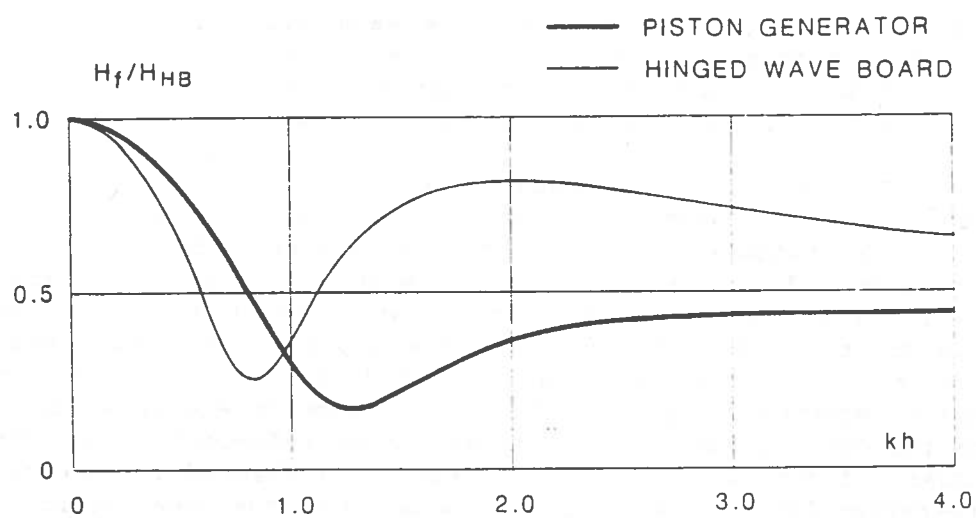

FIGURE 5 RATIO OF FREE WAVE HEIGHT TO BOUND WAVE HEIGHT FOR TWO TYPES OF WAVE GENERATORS

Whereas the free, second harmonic wave produced inadvertently by linear wave generation can be eliminated by use of 2nd-order wave generation, the free wave energy released by the fundamental during reflection can evidently not be avoided.

The free and the bound waves have the same frequency but travel with different phase velocities; the bound wave propagating faster. However, while the free wave propagates at its own celerity, the bound second harmonic wave is locked to the celerity of its fundamental. As a result, the two waves interact differently at different locations in the flume; sometimes causing cancellation, sometimes reinforcement. In other words, the spacial envelope of the second harmonic wave, and consequently of the total non-linear wave oscillates, and it can be shown that the wave length of this variation is:

$$L_x = \frac{c \cdot c_f}{c - c_f} T/2 \tag{9}$$

where c_f is the phase velocity of the free wave with period T/2 and c is the phase velocity of the fundamental wave with period T. In deep water the free wave phase velocity is half that of the fundamental, which means that the length of the envelope oscillations becomes L_x = L/2. If, for example, c_f is only 90% of c, then the length of the envelope oscillation becomes L_x = 4.5 L.

3.3 Numerical Simulation of Wave Reflections

In order to visualize the effect of interaction between the free and bound second harmonics in a wave flume in the presence of reflections, a numerical simulation procedure was developed. This procedure is also applicable to the validation of the non-linear reflection analysis which will be described in Section 3.4.

The simulation procedure permits the specification of the desired fundamental wave height and wave period, the reflection coefficient for the fundamental and the second harmonic component, the length of the flume and the depth of water. With this information the procedure will calculate the water surface variation at any specified location in front of the wave board by superimposing the fundamental incident and reflected waves and their theoretical bound second harmonics as defined by Equations 7 and 8. The second harmonic energy which is bound to the incident fundamental is assumed to be reflected in proportion to the square of the ratio of the incident and reflected fundamental wave. The re-reflection of the reflected wave from the wave board and the natural attenuation of the higher frequency waves during propagation are not included.

As an option, the procedure also permits the simulation of second harmonic, spurious wave energy which results from conventional 1st-order wave generation theory. For simplicity, the piston generator characteristics of Figure 5 are being approximated by:

$$H_f/H_{HB} = \begin{cases} 1 - 0.7\ kh & \text{for } kh \le 1.2 \\ 0.45 - 1/[2(kh)^3] & \text{for } kh > 1.2 \end{cases} \tag{10}$$

Consequently the free second harmonic is approximated by:

$$\eta_f^{(2)}(t) = A^2 \cdot G^+ \cdot (H_f/H_{HB}) \cdot \cos(2\omega t - \phi) \tag{11}$$

where ϕ is approximated as:

$$\phi = \begin{cases} \pi & \text{for } kh \le 0.94 \\ 0.52 + 2.78\ kh & \text{for } 0.94 < kh < 1.88 \\ 5.75 & \text{for } kh \ge 1.88 \end{cases}$$

The above two approximations are considered adequate for the simulation process. As the analysis program must be able to separate the incident and reflected waves of the bound and free components, it is only necessary to know the magnitude of the free wave in the simulation and then assess the analysis program's ability to recover this information.

The results of a simulated example case are given in Figure 6. The wave height of the fundamental is $H^{(1)} = 0.12$ m, the period is $T = 2.0$ s and the water depth is $h = 0.5$ m. From this it has been calculated that the induced 2nd harmonic bound wave is $H_{HB}^{(2)} = 0.026$ m and the associated free wave is $H^2_{(f)} = 0.012$ m. The simulated reflection coefficients are assumed to be: for the fundamental $C_r = 20\%$, for the free 2nd harmonic $C_{r,f} = 30\%$. Figure 6 shows the total wave train at four different positions in the wave flume, i.e. at antinodal points b) and d), and nodal points a) and c). A purely linear wave is also plotted for comparison. The simulation for the wave conditions given above was extended for several locations along the flume from 0 to 12.2 m from the hypothetical first probe. In order to describe how the wave height varies along the length of the flume, one may measure the wave activity either in terms of the height of the wetted surface on the flume wall, (i.e. the wave crest height as observed at a specific location along the flume) or one may measure peak to trough wave heights at the same locations. As described in Section 2.0, either of these methods are used in conventional reflection analysis. Figure 7 shows the result of the former for incident wave height of 0.12 m and 0.06 m. The four cases given in Figure 6 are indicated as solid circles on this graph. Figure 8, on the other hand, gives the same simulation results in terms of the crest to trough wave height measure.

By applying conventional reflection analysis to these two envelope representations one may notice how the second harmonic wave can degrade the accuracy of the reflection measurement. By applying equation (2) with adjacent maximum and minimum envelope values supplied by Figure 7, one may obtain reflection coefficient values ranging between 13% and 23%. This is different from the imposed reflection value of 20% which was successfully recovered by applying equation (2) to the linear

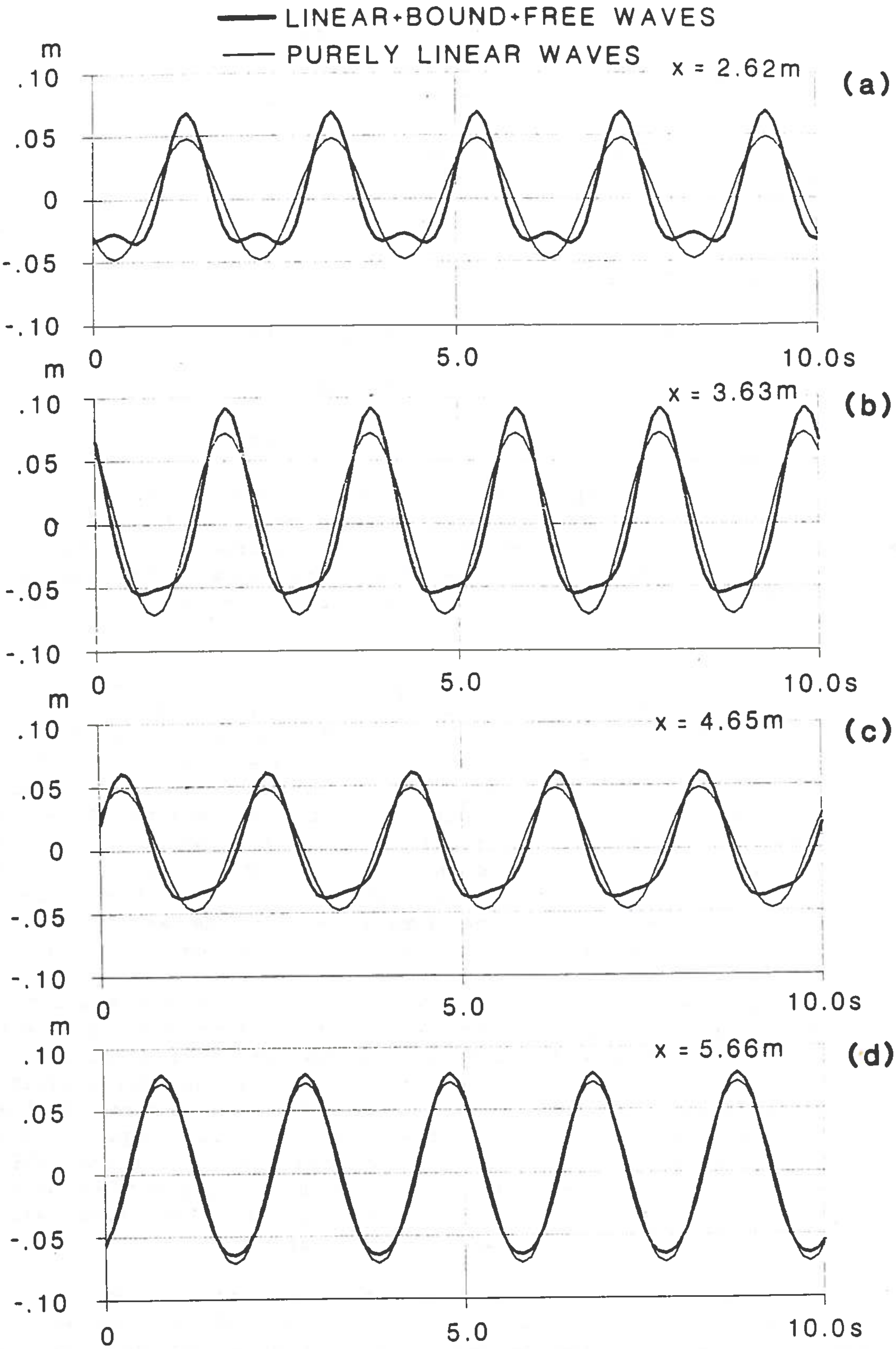

FIGURE 6 TIME SERIES OF CO-EXISTING WAVES AT DIFFERENT FLUME LOCATION USING 1st-ORDER GENERATION

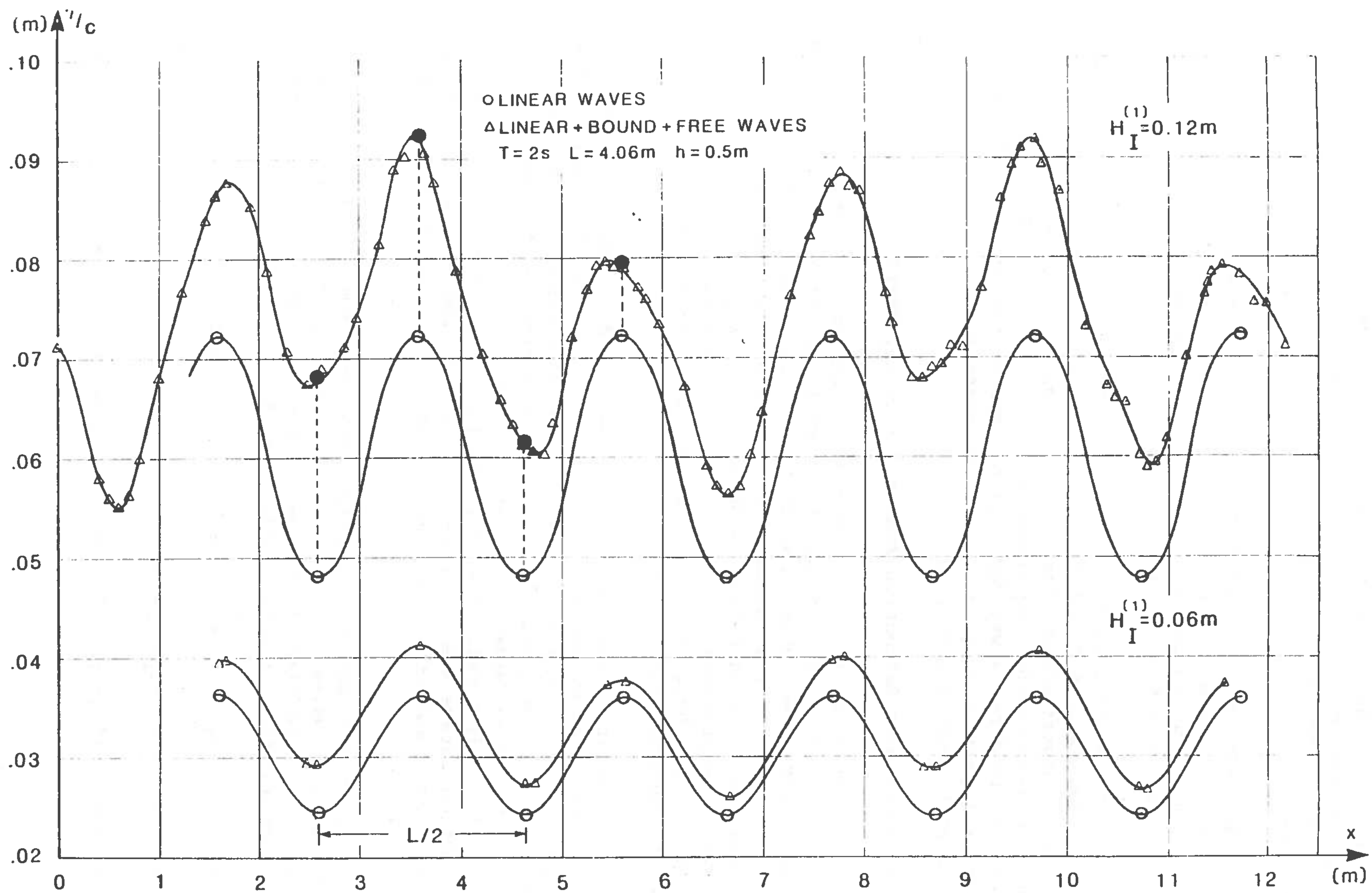

FIGURE 7 VARIATION OF STANDING WAVE ENVELOPE IN LINEAR AND NON-LINEAR WAVES

wave simulation. More dramatic discrepancies can be demonstrated by combining the smallest peak and the largest trough or the largest peak and smallest trough as observed over the total length of the flume as shown in Figure 7.

On the other hand, when the peak to trough wave height is used as provided by Figure 8, rather than the total envelope as shown in Figure 7, then the range of reflection coefficients resulting from equation (2) is only from 17% to 20%.

This second method is evidently more accurate. It will also be noticed from Figures 7 and 8 that the accuracy improves for smaller wave height. Nevertheless, these results cannot be considered in line with modern measurement requirements. The second order reflection analysis described below was designed to improve the accuracy of reflection analysis particularly in situations where a significant amount of second harmonic wave activity exists.

3.4 Non-linear Reflection Analysis Program, REFL2

The program REFL2 is a non-linear approach to the analysis of reflections of regular wave data. As shown in Figure 9, the program requires as inputs the three time series of co-existing waves, namely $\eta_1(t)$, $\eta_2(t)$ and $\eta_3(t)$, as measured by probes p = 1, 2 and 3. The water depth h and the spacings between probes 1 and 2 (X_{12}) and probes 1 and 3 (X_{13}) have to be provided. The outputs of the analysis are the incident and reflected wave heights of the fundamental, and of the bound and the free second harmonic components.

The program uses the Gauss-Newton method to provide an optimal fit in a least squares sense to a sinusoidal function for each of the three wave trains. This supplies then the amplitudes, the frequencies and the phases of the sinusoids which best describe the fundamental component in the three waves. Evidently, the frequency of these three waves should be identical. However, because the present method fits the three function parameters separately to each of the three wave trains, there is a small and in general negligible difference in the optimally fitted frequency.

Given the amplitudes, phases and the common frequency of the three fundamental waves, a reflection analysis by the method described by Mansard and Funke [Ref. 6] can be carried out. This method separates the incident and the reflected fundamental such that for:

$$A_i \cos(\omega t+\phi_i) + A_r \cos(\omega t+\phi_r) + \varepsilon_1(t) = \eta_1(t) \quad (12)$$

$$A_i \cos(\omega t-kX_{12}+\phi_i) + A_r \cos(\omega t+kX_{12}+\phi_r) + \varepsilon_2(t) = \eta_2(t) \quad (13)$$

$$A_i \cos(\omega t-kX_{13}+\phi_i) + A_r \cos(\omega t+kX_{13}+\phi_r) + \varepsilon_3(t) = \eta_3(t) \quad (14)$$

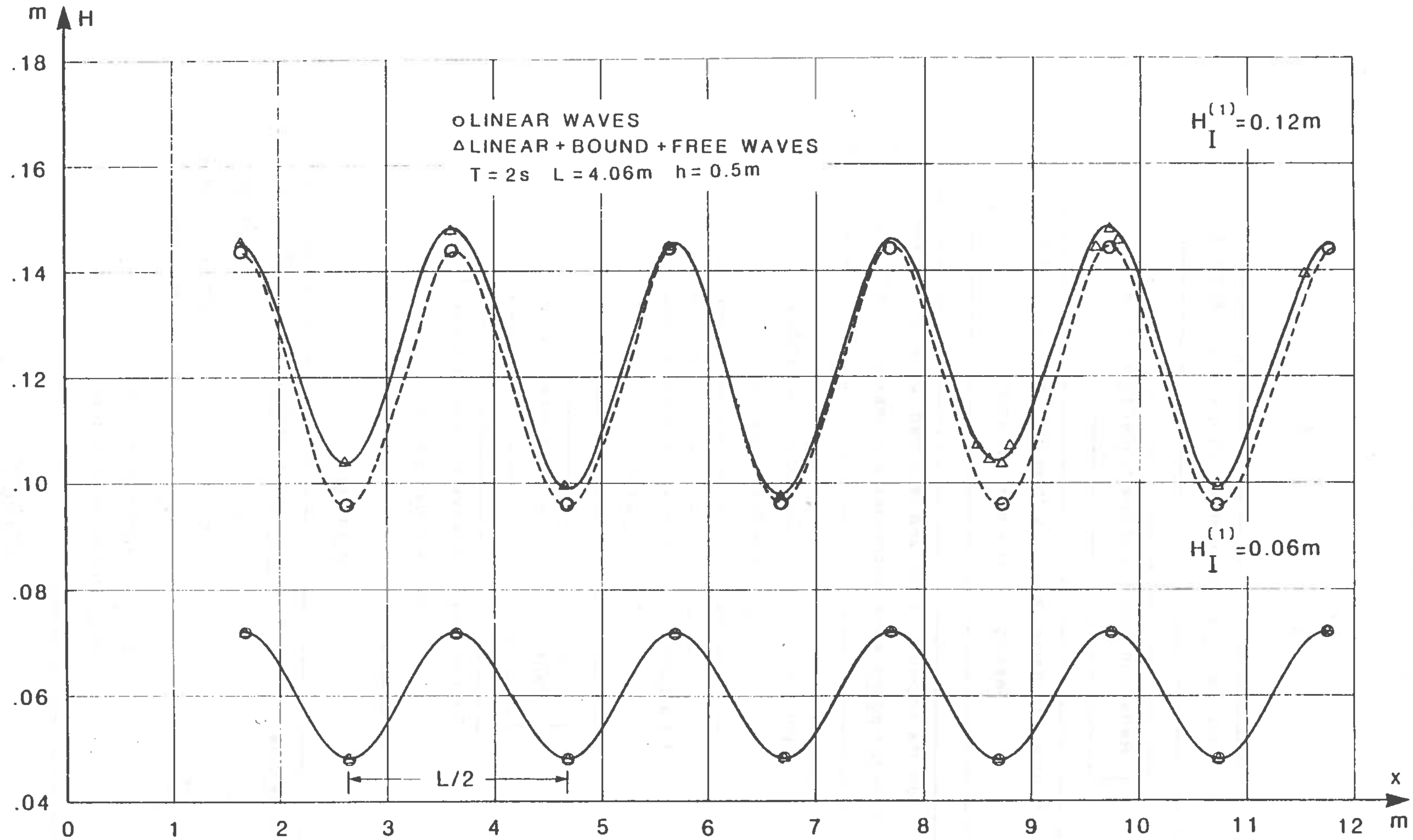

FIGURE 8 VARIATION OF TOTAL HEIGHT IN THE STANDING WAVE SYSTEM IN LINEAR AND NON-LINEAR WAVES

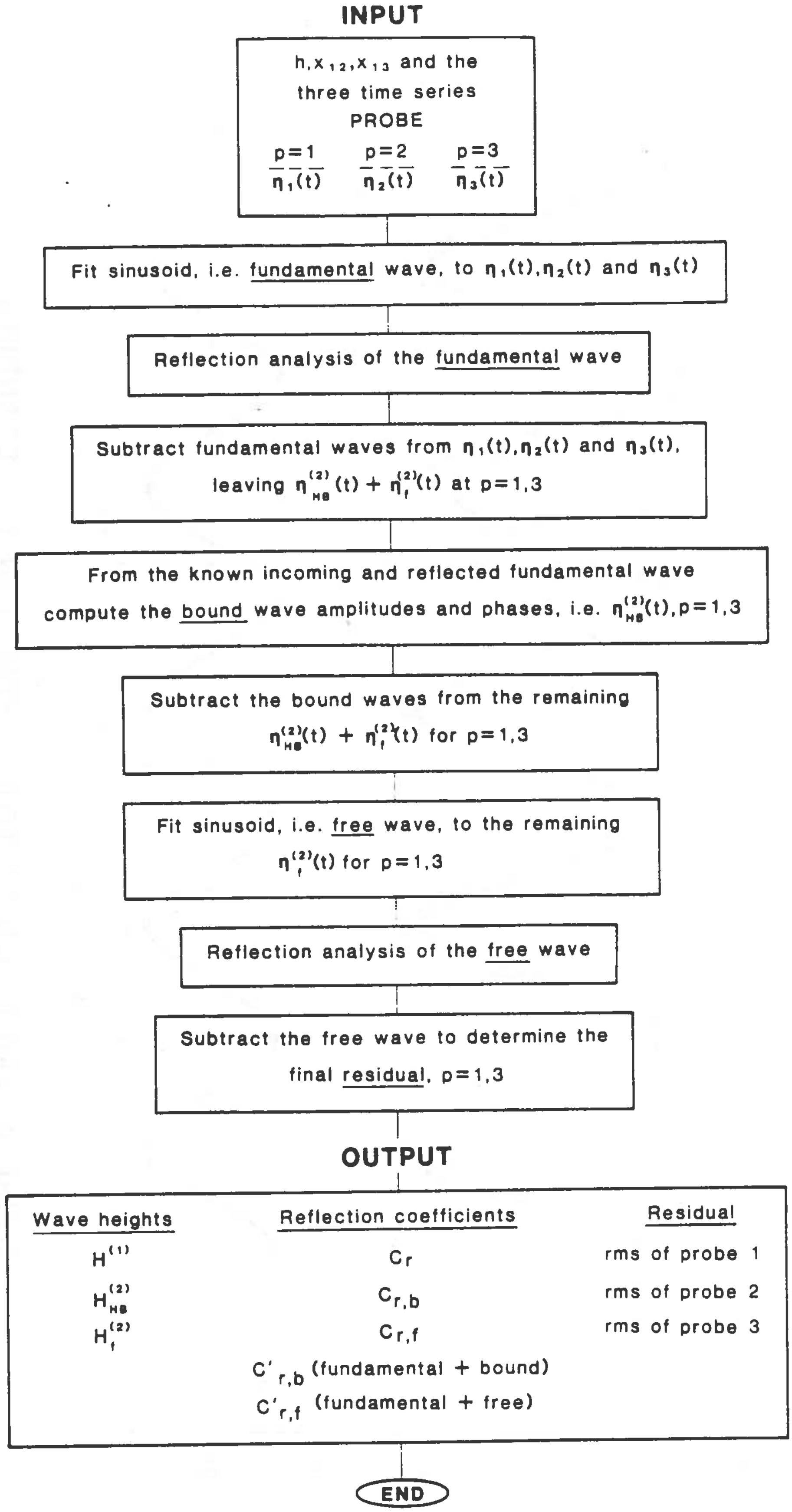

FIGURE 9 FLOW CHART OF REFL2

the sum of the residue squares is a minimum, i.e.

$$\sum_{j=1}^{3} \int_{0}^{T_R} \varepsilon_j^{\,2}(t)\; dt = \text{minimum}$$

The program now subtracts the incident and reflected fundamental components from the three wave records $\eta_1(t)$, $\eta_2(t)$ and $\eta_3(t)$ leaving the three residual functions $\varepsilon_1(t)$, $\varepsilon_2(t)$ and $\varepsilon_3(t)$. These must now contain the second harmonic bound and free components and the noise.

Knowledge of the incident wave height A_i, reflected wave height A_r and their common frequency ω permits the application of Equation (7) to obtain the bound second harmonic wave amplitudes $A_i^{(2)}$ and $A_r^{(2)}$. It is therefore possible to rewrite Equations (12) to (14) as follows:

$$\begin{aligned} A_i \cos(\omega t+\phi_i) &+ A_i^{(2)} \cos(2\omega t+2\phi_i) \\ &+ A_r \cos(\omega t+\phi_r) + A_r^{(2)} \cos(2\omega t+2\phi_r) \\ &\qquad + r_1(t) \;=\; \eta_1(t) \end{aligned} \tag{15}$$

$$\begin{aligned} A_i \cos(\omega t-kX_{12}+\phi_i) &+ A_i^{(2)} \cos(2\omega t-2kX_{12}+2\phi_i) \\ &+ A_r \cos(\omega t+kX_{12}+\phi_r) + A_r^{(2)} \cos(2\omega t+2kX_{12}+2\phi_r) \\ &\qquad + r_2(t) \;=\; \eta_2(t) \end{aligned} \tag{16}$$

$$\begin{aligned} A_i \cos(\omega t-kX_{13}+\phi_i) &+ A_i^{(2)} \cos(2\omega t-2kX_{13}+2\phi_i) \\ &+ A_r \cos(\omega t+kX_{13}+\phi_r) + A_r^{(2)} \cos(2\omega t+2kX_{13}+2\phi_r) \\ &\qquad + r_3(t) \;=\; \eta_3(t) \end{aligned} \tag{17}$$

where $r_1(t)$, $r_2(t)$ and $r_3(t)$ are the residue functions which contain now the free second harmonic components and the noise. These are obtained by subtracting the known bound second harmonic components from the residual functions $\varepsilon_1(t)$, $\varepsilon_2(t)$ and $\varepsilon_3(t)$.

At this point it is possible to apply an additional least squares fitting operation by the Gauss-Newton method to the three residual functions $r_1(t)$, $r_2(t)$ and $r_3(t)$. However, as the frequency of the second harmonic wave is now known to be twice the fundamental frequency, only the amplitude and the phase need to be optimally fitted for each function.

Knowledge of the parameters of the free second harmonic waves at the three probes now permits a separate reflection analysis of these components using the same method as described above. This yields the incident and reflected amplitudes of the free second harmonic wave $A_{i,f}$ and $A_{r,f}$.

The following reflection coefficients can now be computed:

- For the fundamental component we have:

$$C_r = A_r/A_i$$

- For the bound, second harmonic component

$$C_{r,b} = A_r^{(2)}/A_i^{(2)}$$

and since Equation (7) implies that

$$A^{(2)} = (A^{(1)})^2 \cdot G^+$$

it follows that

$$C_{r,b}^{\cdot} = A_r^2/A_i^2 = C_r^2$$

- For the free, second harmonic component

$$C_{r,f} = A_{r,f}/A_{i,f}$$

- For the combined fundamental and bound second harmonic component

$$C_{r,b}' = \left[(A_r^2+A_r^{(2)^2}) \; / \; (A_i^2+A_i^{(2)^2})\right]^{1/2}$$

and finally

- For the combined fundamental and free second harmonic component

$$C_{r,f}' = \left[(A_r^2+A_{r,f}^2) \; / \; (A_i^2+A_{i,f}^2)\right]^{1/2}$$

After removal of the free components from the residuals $r_1(t)$, $r_2(t)$ and $r_3(t)$, the rms values of the remaining noise is also computed. This residual component represents that portion of the measured water surface elevation which cannot be explained by the present 2nd-order theory.

3.5 Test of REFL2 With and Without Noise

The computer program was tested with known, synthesized time series to verify if the incident and reflected waves and the reflection coefficients were computed correctly. In addition to this, it was also of interest to determine the influence of noise on the computed reflection characteristics. The noise was generated according to the description in Section 2.2.

The standing wave system was synthesized for an incident wave height of $H_i^{(1)}$ = 0.12 m, a period of T = 2.0 s, a reflection coefficient of C_r = 20% and a free wave reflection coefficient of $C_{r,f}$ = 30%. The noise level was varied from 0 to 10% of the total incident wave. Table 3 shows the output of the REFL2 analysis. The rms of the final residual is given relative to the rms of the incident wave, i.e. the ratio of the rms is R_{rms} = residual rms/incident rms. The table shows that the output is very stable; even with 10% noise the accuracy of the results is not significantly affected.

Figure 10 illustrates an example of the analysis of a test case without noise. In Figure 10 a) the total wave train is compared to the fit of the basic, fundamental wave. The residue is compared to the computed bound wave in Figure 10 b). In Figure 10 c) the bound wave component has also been subtracted, and the remaining free wave is compared to the fitted one. In Figure 10 d) the final residual is given, which, in this case, is negligible.

Figure 11 shows the output of REFL2 in the case of 10% noise. The residual noise now shows up in Figure 11 d), and it may be seen from Table 3 that the computed residual R_{rms} is 10%, which is exactly the noise level used for the synthesis.

On the basis of this test series it has been demonstrated that REFL2 is capable of decomposing precisely a non-linear wave train into separate incident and reflected parts of fundamental, bound and free waves in spite of the presence of noise.

3.6 Non-linear Reflection Analysis of Flume Data

To further illustrate the use of REFL2 a series of measured flume data were analysed. These were acquired as part of an optimization experiment for a wave absorber. A certain amount of noise is always present in measured wave data, but what was more important in the present case was the deficiency of the wave generator. The machine suffered from backlash as it was noted that the paddle had a tendency to rest a fraction of a second in each extreme position. That is, the regular sinusoidal movement was slightly clipped at the top and the bottom. It is interesting to apply REFL2 to such corrupted data.

Figure 12 shows a fundamental wave of 6.0 s. The profile does not look quite smooth and regular, but the fits to the fundamental, and to the 2nd harmonic bound and the free component seem still reasonable. As seen from Table 4 the reflection coefficient of the fundamental is 46.3%, for the bound it is 21.5%, and for the free wave 22.3%. It has earlier been pointed out that the reflected free waves could consist of reflections of an incident free wave and a contribution from the bound wave energy which may be released as free wave energy in the reflection process.

To demonstrate the possibility that bound, second harmonic waves could be reflected as free second harmonic waves, two additional tests were analysed which have fundamental periods of three seconds, corresponding to the second harmonic period of the first test of Figure 12. It is assumed the two additional tests with fundamental periods of three seconds should reveal the reflective properties of the structure at three seconds. If these second reflection coefficients turn out to be smaller than was found for the first test, then it must be assumed that some of the additional reflected second harmonic energy in the

Noise	$H_i^{(1)}$	$H_{i,HB}^{(2)}$	$H_{i,f}^{(2)}$	$H_r^{(1)}$	$H_{r,HB}^{(2)}$	$H_{r,f}^{(2)}$	C_r	$C_{r,b}$	$C_{r,f}$	$C'_{r,b}$	$C'_{r,f}$	R_{rms}
%	m	m	m	m	m	m	%	%	%	%	%	%
0	0.120	0.026	0.012	0.024	0.001	0.004	20.0	4.0	29.9	19.5	20.0	0
* 0	0.120	0.026	0.012	0.024	0.001	0.004	20.0	4.0	30.1	19.6	20.1	0
1.0	0.120	0.026	0.012	0.024	0.001	0.004	19.9	4.0	30.1	19.5	20.0	1.0
5.0	0.120	0.026	0.012	0.024	0.001	0.004	19.8	3.9	30.7	19.3	19.9	5.0
** 5.0	0.120	0.026	0.012	0.024	0.001	0.004	20.0	4.0	31.5	19.5	20.1	5.0
10.00	0.120	0.026	0.012	0.023	0.001	0.004	20.0	3.8	31.5	19.1	19.7	10.0

* Different location of gauges in flume.
** Based on 2048 data samples.

TABLE 3 RESULTS OF NON-LINEAR REFLECTION ANALYSIS WITH SYNTHESIZED WAVES (C_r = 20%, $C_{r,f}$ = 30%, 1024 data samples)

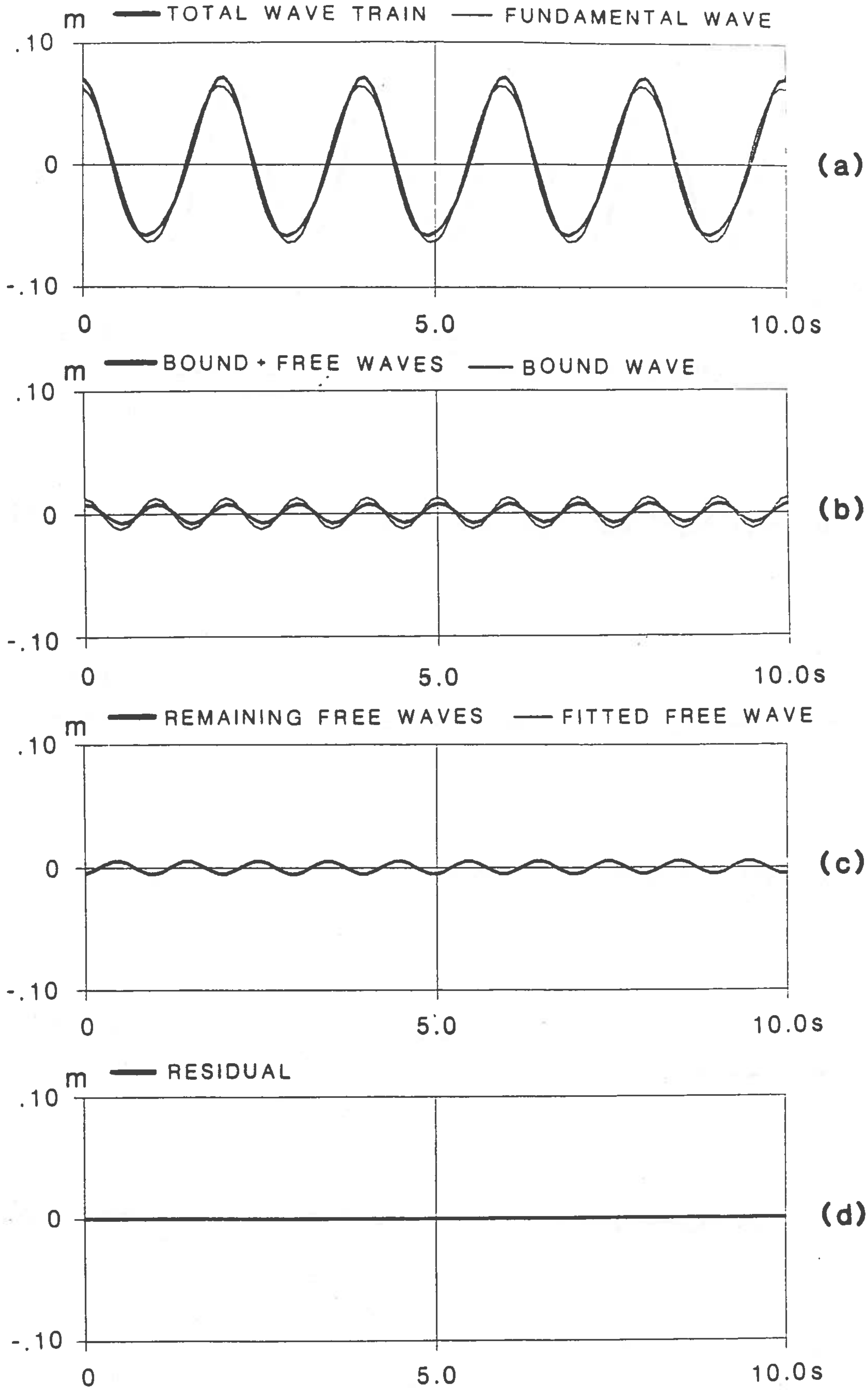

FIGURE 10 TESTING OF REFL2 WITHOUT NOISE

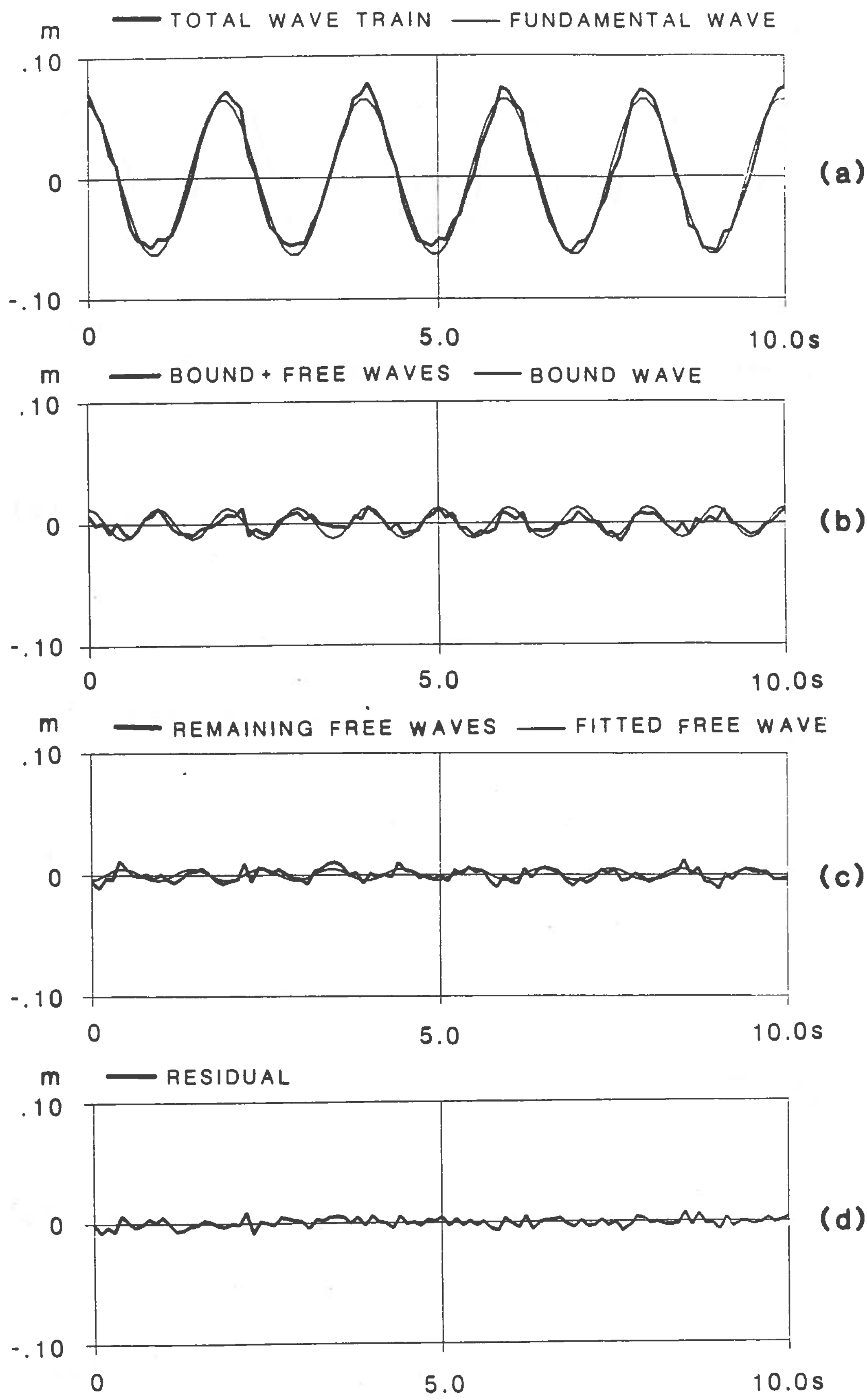

FIGURE 11 TESTING OF REFL2 WITH 10% NOISE

first test came from another source, such as the bound, second harmonic component or from some other non-linear interactions.

Figures 13 and 14 give the results of this additional analysis and it may be noticed from Table 4 that the wave reflection corresponding to Figure 13 is only 13% and corresponding to Figure 14 only 9.6%. As the free second harmonic of Figure 12 has a wave height of approximately 0.03 m and the fundamental wave in Figure 13 of approximately 0.108 m, the comparison is not completely valid. Nevertheless, there is a strong possibility that the test corresponding to Figure 12 reveals some transfer of energy from bound to free second harmonic waves.

The residuals in the Figures 12-14 are seen to be rather substantial, and from Table 4 it also appears that R_{rms} is on the order of 20%. This is not believed to be pure noise. The frequency of the residual in Figures 13 and 14 is very clearly seen to be 1.0 s, i.e. the third harmonic of the fundamental 3.0 s wave. This ties in very well with the behaviour of the wave machine in that a sinusoidal movement with truncated maximum and minimum generates odd harmonics. Therefore, third, fifth, etc. harmonic waves will be present in the flume. However, in the present non-linear analysis technique frequency components above the 2nd harmonic are treated as a noise residual.

3.7 Simulation of Flume Data

The measured 6.0 s wave shown in Figure 12 was generated using traditional 1st-order control of the wave machine. Consequently, free second harmonic spurious waves were being produced. The investigation in this section attempts to simulate the situation by numerical synthesis. The computer procedure described in Section 3.3 was employed for this purpose using the approximations of Equations (10) and (11).

A reflection analysis followed the numerical synthesis of the measured flume data. The results are also shown (bottom line) in Table 4. It was possible to recover the desired reflection coefficient of C_r = 46%. Also the bound and free wave reflection coefficients match the anticipated values well. The measured and simulated profiles are illustrated in Figure 15. The right skew is obviously reproduced. However, the main difference between the wave profiles is that the simulated wave does not include the odd harmonics, which are required to realize the symmetry in the measured wave profile. It can also be seen from Table 4 that only 2.5% real noise was simulated as it was assumed that the rest of the residual energy was contained in third or higher harmonics.

A simulation of the 6.0 s wave using 2nd-order wave generation is described in section 5.1.

4.0 LINEAR ANALYSIS OF NON-LINEAR DATA

To investigate the importance of separating bound and free waves in the reflection analysis a series of non-linear data was analysed with the program REFL3. This program does not distinguish between

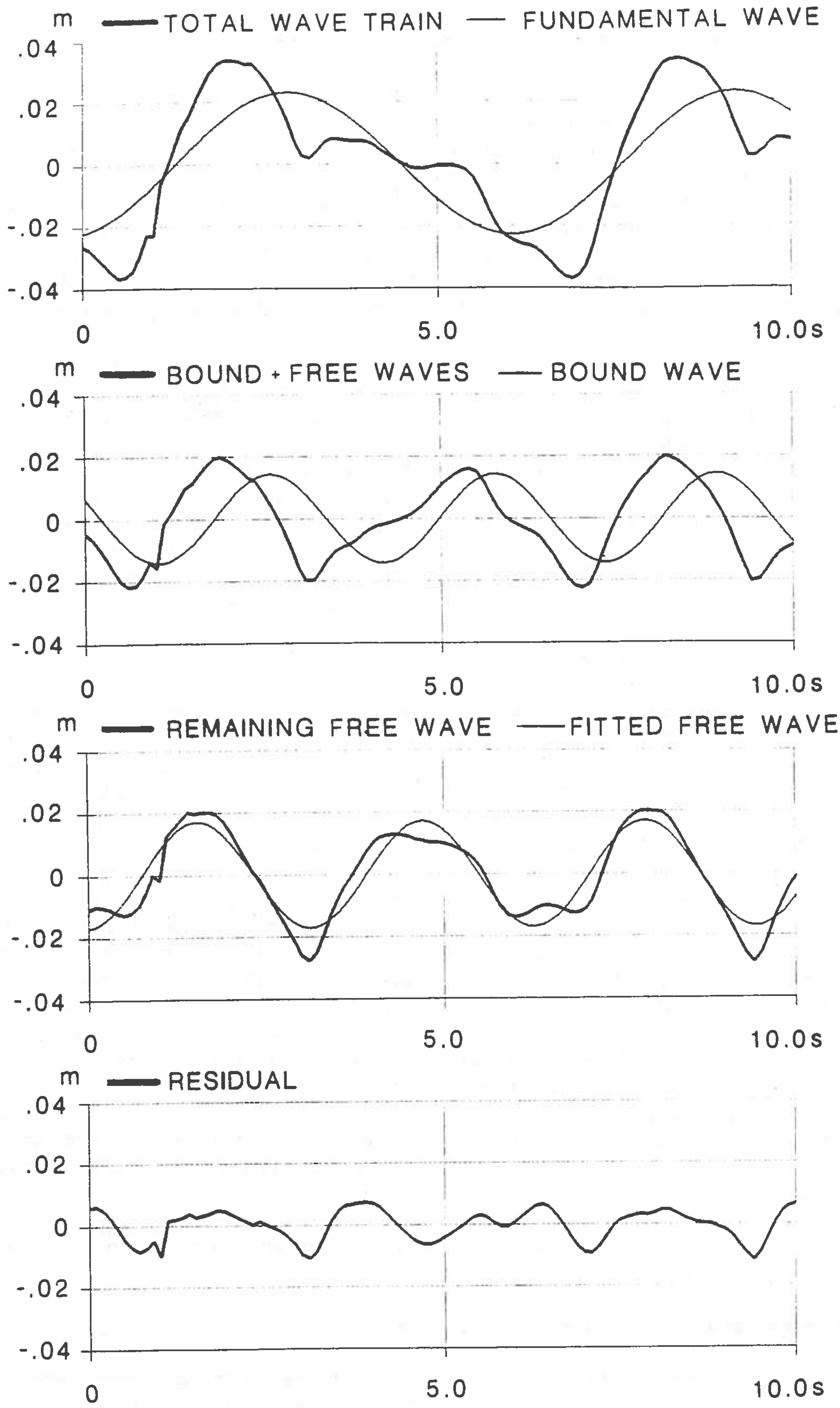

FIGURE 12 ANALYSIS OF T = 6.0s, H = 0.08m WAVE MEASURED IN FLUME

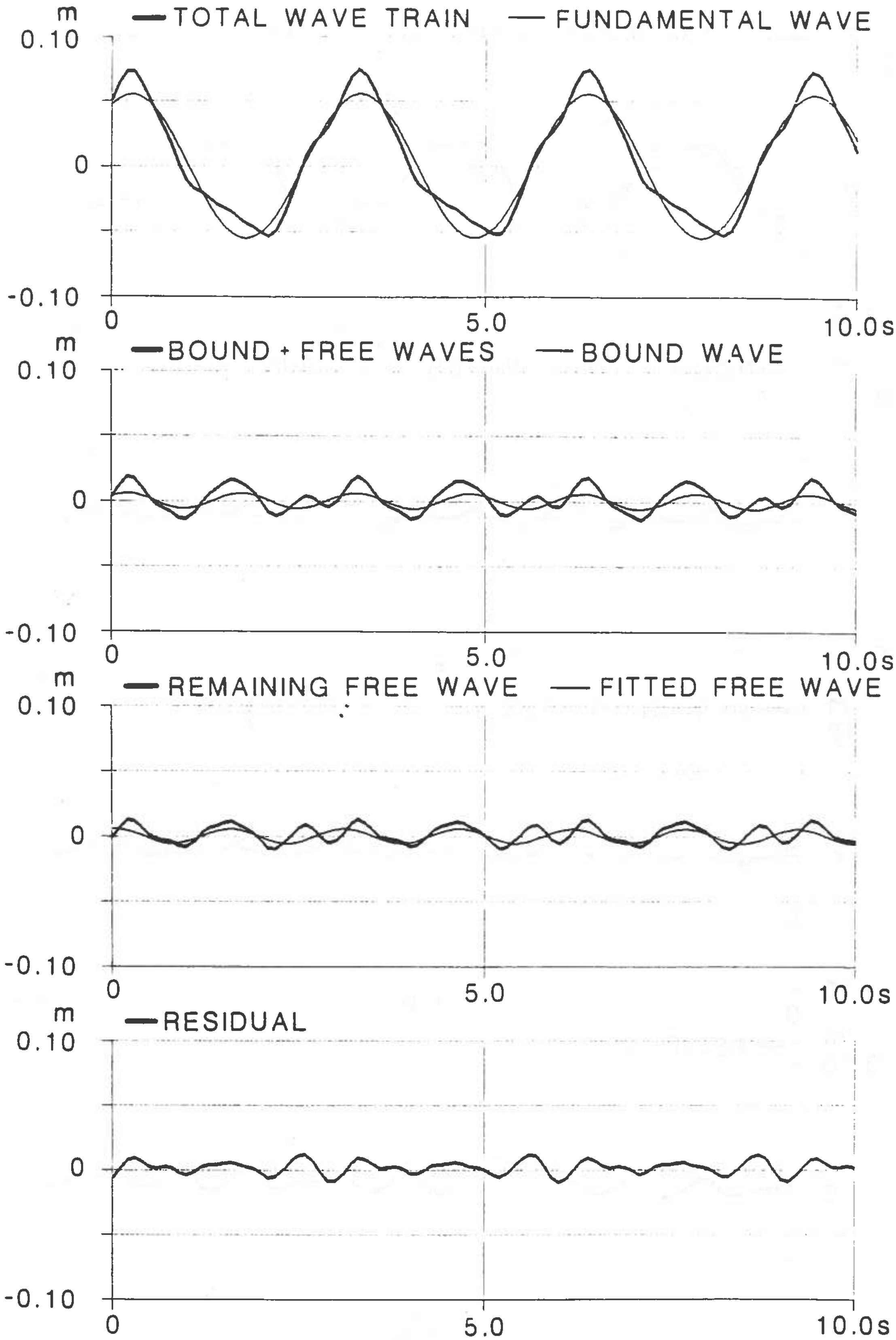

FIGURE 13 ANALYSIS OF T = 3.0s, H = 0.11m WAVE MEASURED IN FLUME

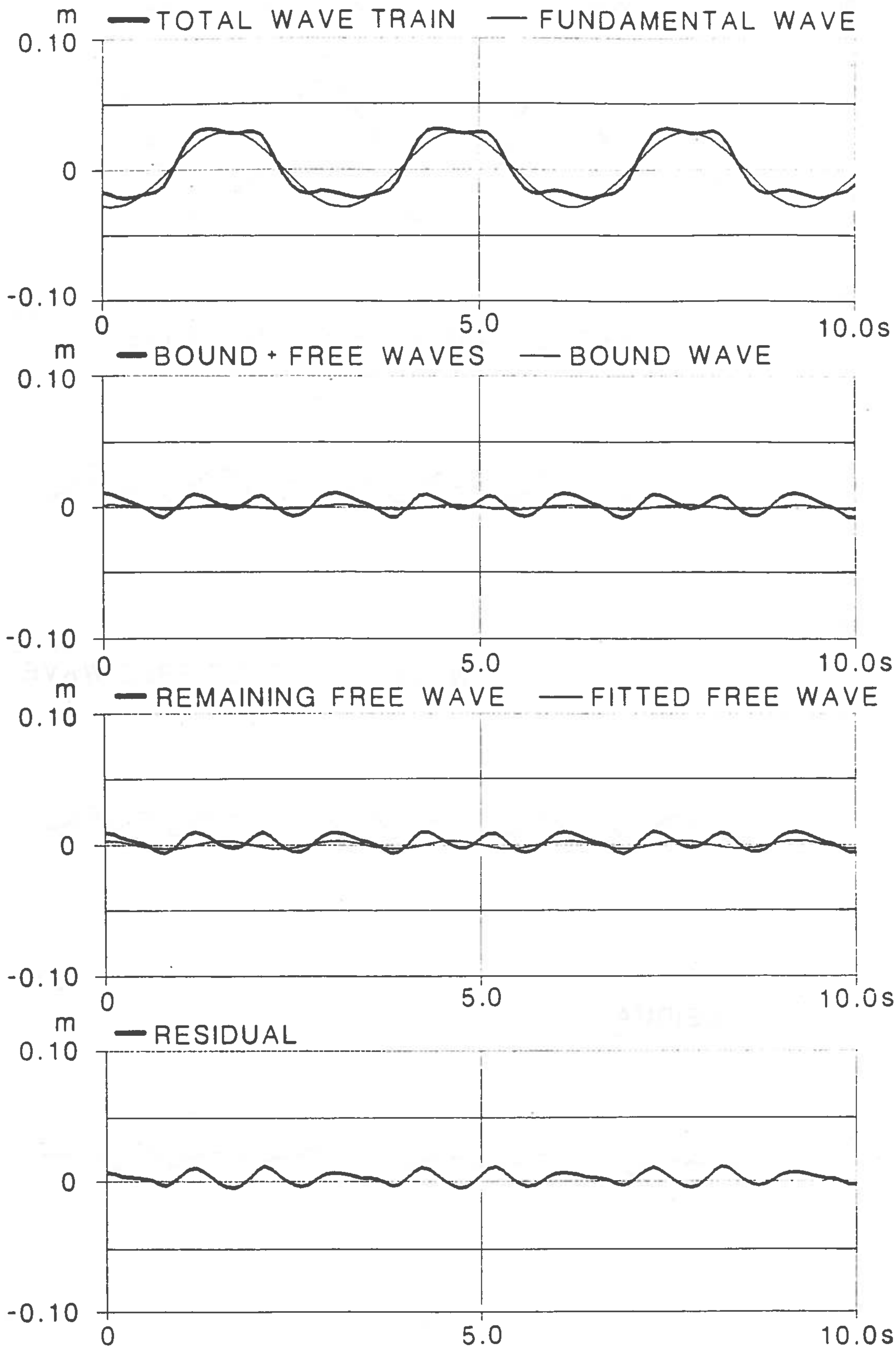

FIGURE 14 ANALYSIS OF T = 3.0s, H = 0.05m WAVE MEASURED IN FLUME

T	$H_i^{(1)}$	$H_{i,HB}^{(2)}$	$H_{i,f}^{(2)}$	$H_r^{(1)}$	$H_{r,HB}^{(2)}$	$H_{r,f}^{(2)}$	C_r	$C_{r,b}$	$C_{r,f}$	R_{rms}
s	m	m	m	m	m	m	%	%	%	%
6.0	0.079	0.024	0.028	0.037	0.005	0.006	46.3	21.5	22.3	21.0
3.0	0.108	0.012	0.012	0.014	0.000	0.001	13.0	1.7	8.0	15.7
3.0	0.054	0.003	0.004	0.005	0.000	0.002	9.6	0.9	50.0	28.1
* 6.0	0.079	0.024	0.018	0.036	0.005	0.004	45.8	20.9	21.8	2.5

* Numerically simulated.

TABLE 4 ANALYSIS OF MEASURED FLUME DATA

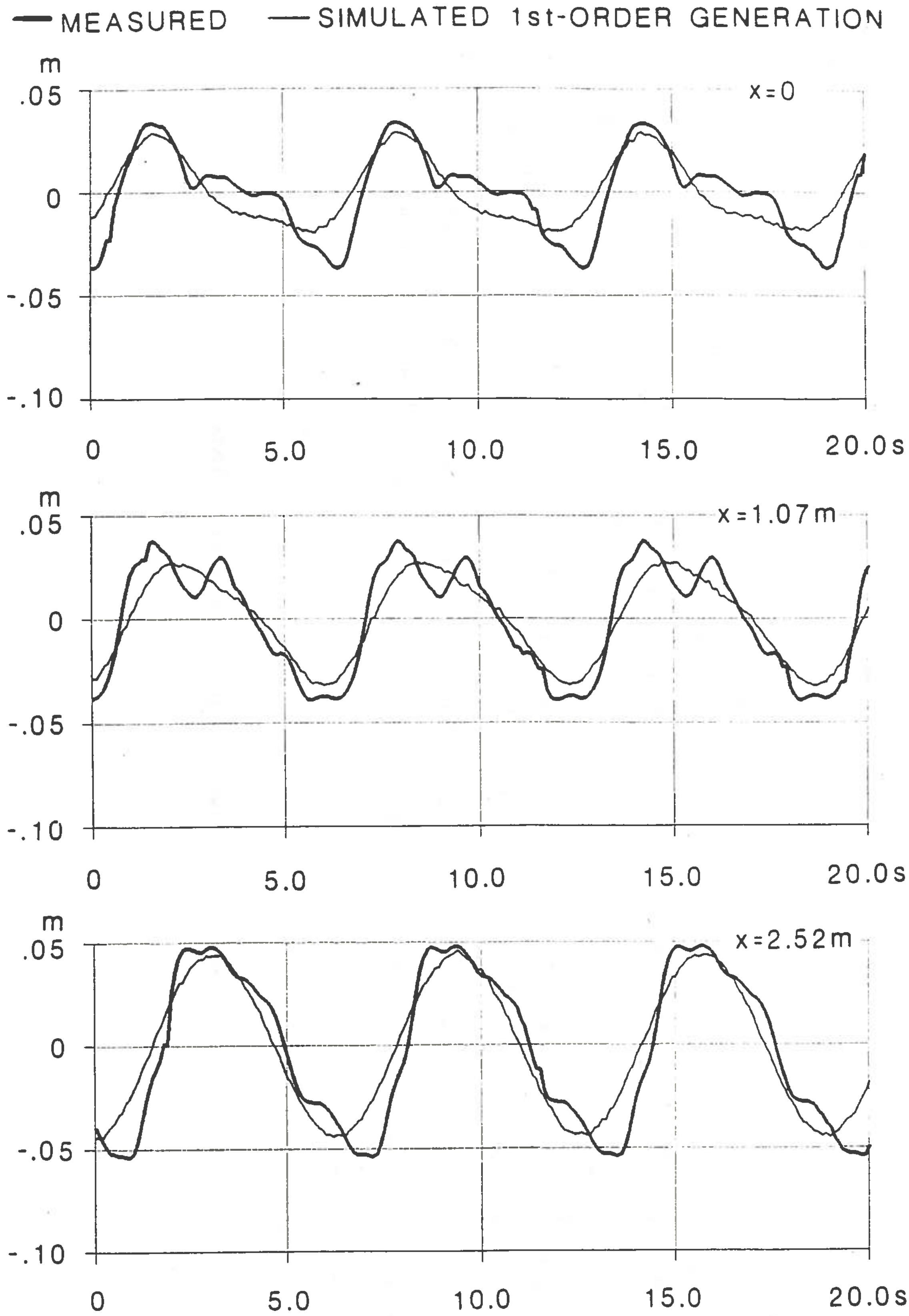

FIGURE 15 NUMERICAL SIMULATION OF REFLECTION WITH T= 6.0s WAVE USING 1st-ORDER GENERATION

free and bound waves, i.e. the program assumes all waves to be free and linear. A comparison of the output of REFL2 and REFL3 is given in Table 5.

For the first wave with T = 3.0 s, REFL3 seems to output free second harmonic wave quantities, which are approximately the sum of the bound and free second harmonic waves. This is also the case for the second T = 3.0 s wave, but it should be noted that in this case the amplitudes are very small, which could make the results suspicious. However, for case three and four, i.e. with T = 6.0 s waves, there are significant differences between the results of REFL2 and REFL3. The latter gives a much smaller free wave amplitude than the sum of the second harmonic bound and free waves, and the reflection coefficients are also different. The reasons for this may be that at some of the wave gauges, the phase of the second harmonic bound and that of the second harmonic free wave cancel to a certain extent. REFL3 can only interpret that as a reduced wave amplitude. The calculation of the reflection coefficients will therefore be affected. The same effect seems to apply also to the last two cases in Table 5, i.e. the T = 2.0 s waves.

The conclusion of these tests as outlined in Table 5 seems to be that it is rather important to distinguish between bound and free second harmonic waves in the reflection analysis of non-linear regular waves.

5.0 SECOND-ORDER WAVE GENERATION

The non-linear character of a regular wave with its higher harmonic component implies that a conventional linear control signal based on Biesel's transfer function [Ref. 1], will be insufficient for a correct generation. To find the proper wave board control signal the Laplace equation and the paddle boundary condition have to be expanded to 2nd order, c.f. Sand and Mansard [Ref. 10], and Flick and Guza [Ref. 4]. The solution is a non-linear correction to the traditional 1st-order signal. Thus, generation of the regular wave in equation (6) requires first the basic linear signal:

$$X^{(1)}(t) = A \frac{\sinh(kh)\ \cosh(kh)+kh}{2\ \sinh^2(kh)} \sin(\omega t) \tag{20}$$

and in order to secure a proper reproduction of the higher harmonic in equation (7), the following 2nd-order signal has to be superimposed:

$$X^{(2)}(t) = A^2\ F_1\ \sin(2\omega t) + A^2\ F_{23}\ \cos(2\omega t) \tag{21}$$

in which F_1 and F_{23} are rather complicated transfer functions described in Sand and Mansard [Ref. 10].

As indicated above, the use of the 2nd-order control signal implies that only the regular wave and its higher harmonic component

REFL2								REFL3						
T	$H^{(2)}_{i,HB}$	$H^{(2)}_{i,f}$	$H^{(2)}_{r,HB}$	$H^{(2)}_{r,f}$	$C_{r,b}$	$C_{r,f}$	$C'_{r,f}$	$H^{(2)}_{i,HB}$	$H^{(2)}_{i,f}$	$H^{(2)}_{r,HB}$	$H^{(2)}_{r,f}$	$C_{r,b}$	$C_{r,f}$	$C'_{r,f}$
s	m	m	m	m	%	%	%	m	m	m	m	%	%	%
a) 3.0	0.012	0.012	0.000	0.001	1.7	8.0	13.0	0	0.024	0	0.003	0	10.7	12.9
a) 3.0	0.003	0.004	0.000	0.002	0.9	50.0	10.2	0	0.007	0	0.002	0	34.6	10.4
a) 6.0	0.024	0.028	0.005	0.006	21.5	22.3	44.3	0	0.025	0	0.006	0	24.3	44.8
b) 6.0	0.024	0.018	0.005	0.004	20.9	21.8	44.9	0	0.008	0	0.007	0	93.6	46.5
c) 2.0	0.026	0.012	0.001	0.004	4.0	29.9	20.0	0	0.016	0	0.005	0	33.5	20.3
d) 2.0	0.026	0.012	0.001	0.004	3.8	31.5	19.7	0	0.016	0	0.005	0	34.4	19.9

a) Measured wave data. b) Simulated case. c) Synthesized, no noise. d) Synthesized, 10% noise.

TABLE 5 COMPARISON BETWEEN NON-LINEAR AND LINEAR ANALYSIS OF NON-LINEAR WAVE DATA

will be generated. If, however, attempts are made to generate the same wave with only the 1st-order control signal, an additional undesired free higher harmonic wave will appear in the flume. This free wave component has been briefly discussed in section 3.2.

5.1 Numerical Simulation with 2nd-order Generation

In Figure 6 the non-linear waves appearing as a result of 1st-order wave generation were simulated. For comparison a simulation of the correct use of 2nd-order control signals is presented in Figure 16. The purely linear waves are compared to the sum of linear and bound (no free) waves. The characteristic flat troughs and sharp crests appear. The fundamental wave height is $H^{(1)} = 0.12$ m, and this case can also be compared to Figures 7 and 8. First of all, it is seen that the nodes, a) and c), and the antinodes, b) and d), do not vary along the flume like they do for the wave of Figure 6. Thus, in the present case both the envelope and the crest-trough method would work satisfactorily, i.e. they would return the $C_r = 0.20$. This in itself shows the advantage of using a 2nd-order wave generation method.

A further application of 2nd-order wave generation is presented in Figure 17, which relates to the simulation of flume data described in Section 3.7. The measured data shown in Figure 15 are now compared to the wave profiles obtained by 2nd-order wave generation. This means that the fundamental and bound second harmonic waves were maintained, but the free second harmonic was completely suppressed. It is clearly evident that the agreement is poorer than in Figure 15. This seems to confirm that the measured data were really produced by a 1st-order control signal. Apart from the discrepancies caused by third (and higher) harmonics produced inadvertently by the backlash in the machinery it appears that both the 1st and the 2nd-order simulation programs produce reasonable results.

6.0 SOURCES OF INACCURACIES

A certain amount of noise and measurement errors are always present in laboratory flumes or basins. In cases where the amplitude of the waves is very small, the ratio of noise/signal can become high and cause inaccuracies in the estimation of reflection. Hence, when dealing with waves which are very small in height, the reflection coefficient must be treated with caution (see Table 1 for the effect of noise).

Another source of inaccuracy could appear when the waves are of large amplitude. In the reflection analysis, it is assumed that both incident and reflected fundamental components travel according to the linear dispersion relation, and the net phases between each probe are therefore determined by this. But it is shown by Cokelet [Ref. 2] and Rienecker and Fenton [Ref. 3] that waves with large steepness travel faster than predicted by linear theory. For waves close to critical steepness ($0.14 \tanh 2\pi h/L$), they could propagate up to 18% faster in deep water, and in shallow water even higher (30%). However, it must be stressed that these critical steepnesses represent extreme conditions which are not commonly encountered in laboratory tests. For waves of average steepness it may be that the accuracies provided by the linear

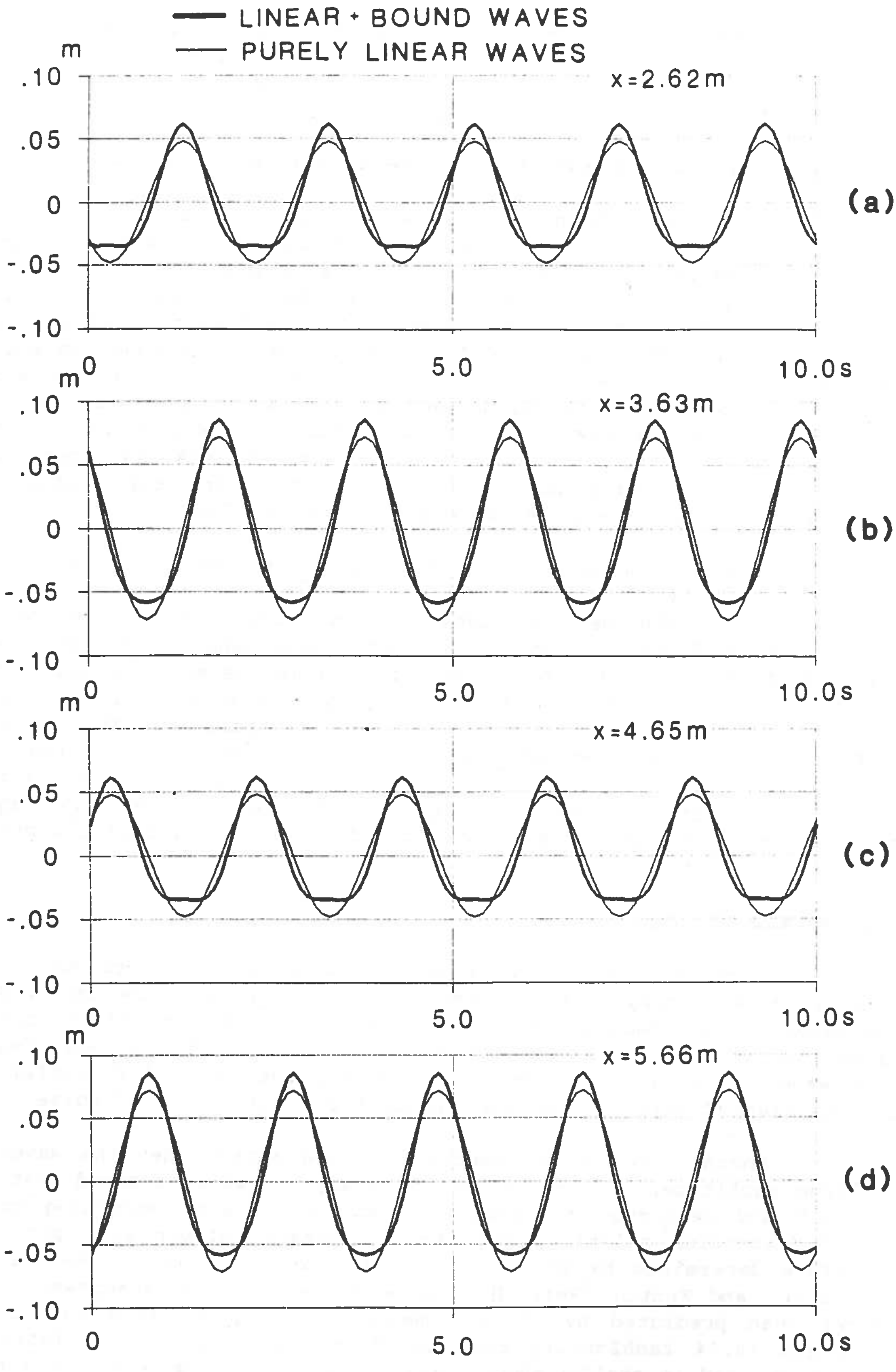

FIGURE 16 TIME SERIES OF CO-EXISTING WAVES AT DIFFERENT FLUME LOCATIONS USING 2nd-ORDER GENERATION

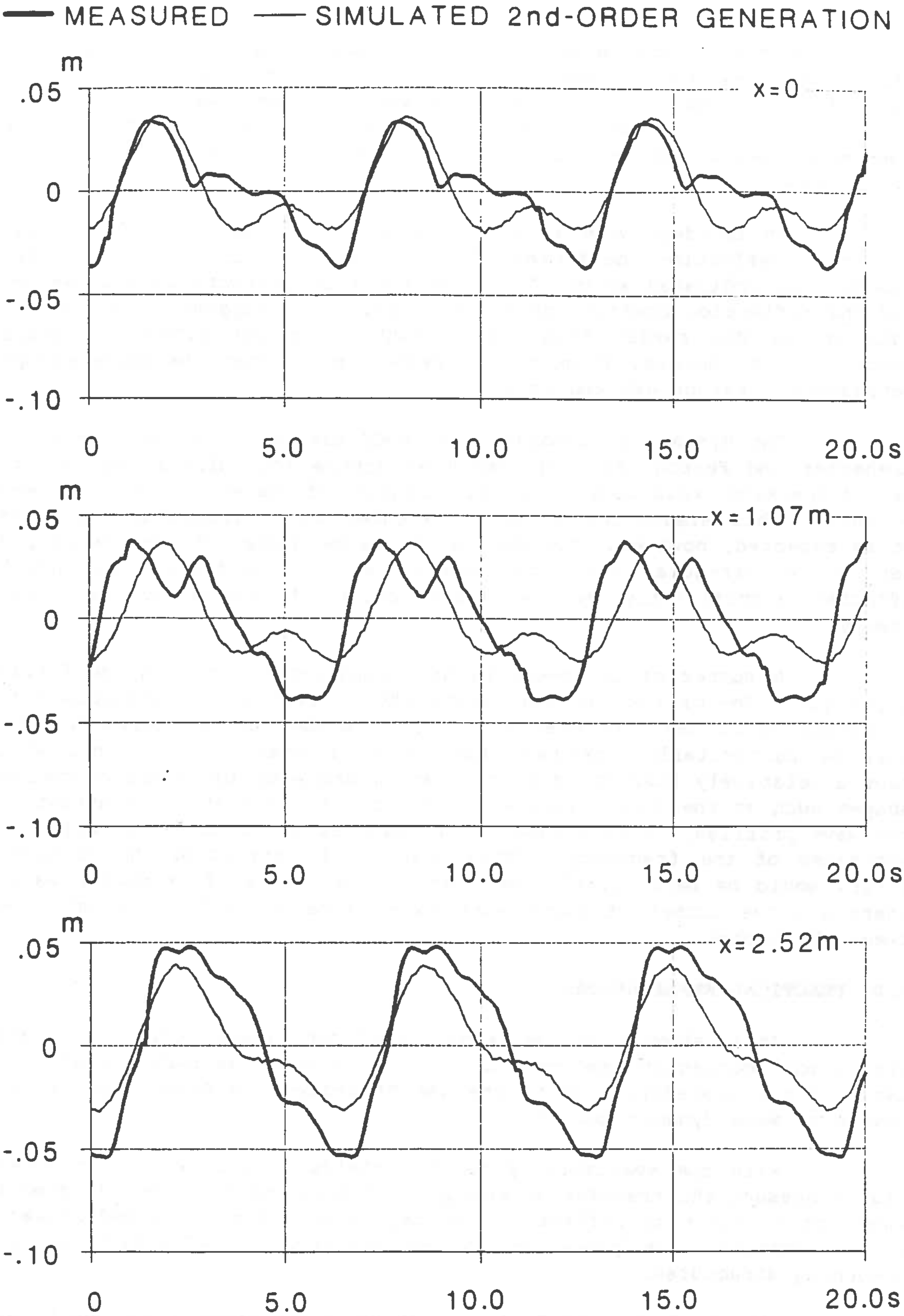

FIGURE 17 NUMERICAL SIMULATION OF REFLECTION WITH T = 6.0s WAVE USING 2nd-ORDER GENERATION

dispersion theory are acceptable. However, to study this particular effect of non-linear dispersion, a special numerical simulation was carried out. For this purpose, the incident wave was assumed to be propagating at 1.1 times the linear celerity, while the reflected component, being smaller in height, was assumed to correspond to the linear theory.

An incident wave of height 12 cm and period 2 s was synthesized with a reflection coefficient of 20%. The reflection analysis which assumes, as indicated above, linear propagation characteristics, estimated the reflection coefficient to be 17.9%. This suggests that appreciable errors can result from the assumption of the linear dispersion theory. Nevertheless, it must be stressed again that the above example represents a rather extreme case.

The Hydraulics Laboratory of NRCC has recently implemented the Rienecker and Fenton [Ref. 3] numerical scheme for calculating non-linear dispersion relations over all ranges of water depths and wave heights. This simulation is being extended to an irregular sea state. It is expected, however, that due to the large number of components present in an irregular sea, the mean reflection coefficient may not be affected significantly by the introduction of non-linear dispersion theory.

A number of improvements are being implemented in the fitting technique. One of them is the capability of fitting simultaneously the frequency which best represents the three probes being analysed. This will be particularly important for waves of small wave height, which have a relatively high noise/signal ratio, and also for waves of cnoidal shapes such as the ones presented in Figure 15. The strong contrasts of the wave profiles, in this case, could have easily resulted in different estimates of the frequency. This feature of optimizing the frequency first, would be particularly important for analysis of irregular waves, where a large number of components have to be properly correlated between the probes.

7.0 PRACTICAL APPLICATIONS

It is shown that the technique of non-linear reflection analysis is more convenient and more accurate than other methods currently in use. It may therefore promote the use of reflection measurement in the course of wave dynamic testing.

With the availability of this analysis tool (which can potentially measure the transfer of energy from bound to free second harmonic waves as a result of reflection) it may be possible to extend research in the physical wave processes in the vicinity of reflective or wave absorbing structures.

The present method of analysing reflections with non-linear regular waves can be seen as the forerunner of a more general principle dealing with irregular wave trains. The basic idea can definitely be transferred to the case of a large number of frequencies, which interact non-linearly and each of which individually carries a 2nd harmonic component. With the many components of different bound and free harmonics comprising an irregular wave train, it is likely that the overall results of the reflection analysis may show more of a difference between linear and non-linear analysis techniques.

It is also suggested that the technique of separating bound and free components could be extended to the group bound long waves although this applies only to the irregular wave situation. However, in practice it is more difficult to measure long wave reflections because the participating wave probes must be spaced much further apart than is required for short waves.

8.0 CONCLUSIONS

An improved technique for linear and non-linear reflection analysis for regular waves has been presented. Both methods are based on a non-linear least squares curve fit of sinusoidal functions to measured wave trains acquired from three wave probes.

The non-linear reflection analysis is capable of separating the bound and free second harmonic components from the total wave train permitting the reflection analysis of each of these components.

Numerical simulations used for the validation of the reflection analysis programs were applied to the synthesis of the standing wave envelope. From this it was determined that the traditional method of reflection analysis by the envelope method is subject to errors and is certainly dependent on the choice of measurement location within the flume. If an envelope must be used, then the method of measuring crest to trough wave heights at the node and the antinode is more accurate than the measurement of the envelope of the wetted surface. In either case significant improvements in measurement accuracy can be obtained if the generation of spurious second harmonic free waves is suppressed by the application of 2nd-order wave generator theory.

The new method is found to be quite insensitive to significant amounts of co-existing noise and can analyse records of arbitrary length without loss of accuracy.

9.0 REFERENCES

1. Biesel, F. "Étude théorique d'un type d'appareil à houle". La Houille Blanche, 6^{e} Ann., No. 2, 1951, pp. 152-165.

2. Cokelet, E.D. "Steep Gravity Waves in Water of Arbitrary Uniform Depth". Phil. Trans., R. Soc., Vol. 286, 1977, pp. 183-230.

3. Rienecker, M.M. Fenton, J.D. "A Fourier Approximation Method for Steady Water Waves". Journal of Fluid Mech., Vol. 104, 1981, pp. 119-137.

4. Flick, R.E.
Guza, R.T.
"Paddle Generated Waves in Laboratory Channels".
J. Waterway, Port, Coastal and Ocean Division, ASCE, Vol. 106, No. WW1, 1980, pp. 79-97.

5. Goda, Y.
Suzuki, Y.
"Estimation of Incident and Reflected Waves in Random Wave Experiments".
Proc. 15th Coastal Engineering Conference, Honolulu, Hawaii, 1976.

6. Mansard, E.P.D.
Funke, E.R.
"The Measurement of Incident and Reflected Spectra Using a Least Squares Method".
Proc. 17th Coastal Engineering Conference, Sydney, Australia, 1980.

7. Mansard, E.P.D.
Funke, E.R.
"On the Reflection Analysis of Two-Dimensional Irregular Waves".
National Research Council of Canada, Hydraulics Laboratory Technical Report, 1986, to be published.

8. Morden, D.B.
Richey, E.P.
Christensen, D.R.
"Decomposition of Co-existing Random Wave Energy".
Proc. 15th Coastal Engineering Conference, Honolulu, Hawaii, 1976.

9. Sand, S.E.
"Long Wave Problems in Laboratory Models".
J. Waterways, Port, Coastal and Ocean Division, Proc. ASCE, Vol. 108, No. WW4, 1982, pp. 492-503.

10. Sand, S.E.
Mansard, E.P.D.
"Reproduction of Higher Harmonics in Irregular Waves".
National Research Council of Canada, Hydraulics Laboratory Technical Report, TR-HY-012, 1985.

11. Stokes, G.G.
"On the Theory of Oscillatory Waves".
Transactions of the Cambridge Philosophical Society, Cambridge, England, Vol. 8, 1847, pp. 441-455.

12. Thornton, E.B.
Calhoun, R.J.
"Spectral Resolution of Breakwater Reflected Waves".
Journal ASCE Waterways, Harbour and Coastal Engineering, WW4, 1972.

REPORT DOCUMENTATION PAGE/PAGE DE DOCUMENTATION DE RAPPORT

REPORT/RAPPORT	REPORT/RAPPORT
TR-HY-011 (1a)	(1b)
REPORT SECURITY CLASSIFICATION / CLASSIFICATION DE SÉCURITÉ DE RAPPORT: UNCLASSIFIED (2)	DISTRIBUTION/DIFFUSION: UNLIMITED (3)

TITLE/SUBTITLE/TITRE/SOUS-TITRE (CLASSIFICATION)

Reflection Analysis of Non-linear Regular Waves

4

AUTHOR(S)/AUTEUR(S)

E.P.D. Mansard, S.E. Sand and E.R. Funke

5

SERIES/SÉRIE

Technical Report

6

CORPORATE AUTHOR/PERFORMING AGENCY/AUTEUR D'ENTREPRISE/AGENCE D'EXÉCUTION

Hydraulics Laboratory, Division of Mechanical Engineering

7

SPONSORING AGENCY/AGENCE DE SUBVENTION

8

DATE	FILE/DOSSIER	LAB. ORDER / COMMANDE DU LAB.	PAGES	DIAGS	REFS
1985/11			46	17	12
9	10	11	12a	12b	12c

NOTES

13

DESCRIPTORS(KEY WORDS)/MOTS-CLÉS

Higher harmonics, regular/irregular waves, non-linear wave equations, free harmonic waves, reflection analysis.

14

SUMMARY/SOMMAIRE

A reflection analysis technique based on optimal fitting of sinusoids is described for regular waves. A non-linear approach has been used to distinguish the bound and free components for waves of finite amplitude. Validation of this technique has been carried out by extensive numerical simulations.

15

ADDRESS/ADRESSE

J. Ploeg, Hydraulics Laboratory,
Division of Mechanical Engineering,
Montreal Rd., Ottawa, Ontario, K1A 0R6, Canada
Telephone: (613) 993-2417

16